[DESCRIPTION]

[Title of Invention] PEPTIDE DERIVATIVE AND PHARMACEUTICAL COMPOSITION CONTAINING SAME

[Technical Field]

[0001]

The present invention relates to peptide derivatives useful in cancer therapy, and pharmaceutical compositions comprising the same.

The present application claims the benefit of Japanese Patent Application No. 2017-140101, filed on July 19, 2017, the entire contents of which are incorporated herein by reference.

[Background Art]

[0002]

Estrogen-receptor α (ERα) plays a key role in the development and progression of breast cancer. The current endocrine therapies for breast cancer mainly target ERα signaling, and use selective ERα modulators (for example, tamoxifen and raloxifene), ERα down-regulators (for example, fulvestrant), and aromatase inhibitors (AI) (NPLs 1 to 3). Among these therapies, a method that uses tamoxifen, which inhibits breast cancer cell proliferation through competitive binding to ERα, is a standard therapy for patients with ERα-positive breast cancer. However, tamoxifen therapy is often ineffective, and the patient may die from recurrent endocrine therapy-resistant tumors (NPLs 4 and 5). Furthermore, compared with tamoxifen, AI, which blocks estrogen synthesis, provides substantial clinical effects such as good efficacy, significant increase in relapse-free survival period, and a prolonged time to disease recurrence in postmenopausal women; however, some patients who have undergone AI treatment still relapse (NPLs 6 and 7). The precise molecular events having effects on the efficacy of these endocrine therapies remain unknown.

[0003]

A complex formed between brefeldin A-inhibited guanine nucleotide-exchange protein 3 (BIG3), which is a cancer specific protein, and prohibitin 2 (PHB2), which is a tumor suppressor, plays a key role in estrogen signaling regulation in ERα-positive breast cancer (NPLs 8 and 9). BIG3 binds to PHB2 to inhibit the ability of PHB2, which suppresses the estrogen-dependent transcriptional activation, and thereby causes constitutive ERα activation.

Based on these findings, strategies of making PHB2 exhibit its tumor suppressive activity by dissociating PHB2 from its complex with BIG3 through inhibition of the BIG3-PHB2 interaction, may become a novel therapy for breast cancer. Based on this strategy, the present

inventors have previously developed a dominant negative peptide of BIG3, which specifically inhibits the BIG3-PHB2 interaction (PTL 1). This peptide has been confirmed to suppress breast cancer growth by reactivating the tumor suppressive activity of PHB2 to inhibit ERα-signaling pathways that bring about the growth of breast cancer (PTL 1).

[Citation List]

[Patent Literature]

[0004]

[PTL 1] WO 2013/018690

[Non-patent Literature]

[0005]

[NPL 1] Johnston, S. R., Clin. Cancer Res. 16, 1979-1987 (2010).
[NPL 2] Fisher, B. *et al.*, J. Natl. Cancer Inst. 97, 1652-1662 (2005).
[NPL 3] Jordan, V. C., Nature Rev. Drug Discov. 2, 205-213 (2003).
[NPL 4] Clarke, R. *et al.*, Pharmacol. Rev. 53, 25-71 (2001).
[NPL 5] Fisher, B. *et al.*, J. Natl. Cancer Inst. 93, 684-690 (2001).
[NPL 6] Chlebowski, R. *et al.*, Breast 2, S1-11 (2009).
[NPL 7] Chumsri, S. *et al.*, J. Steroid Biochem. Mol. Biol. 125, 13-22 (2011).
[NPL 8] Kim, J. W. *et al.*, Cancer Sci. 100, 1468-1478 (2009).
[NPL 9] Yoshimaru, T. *et al.*, Nat. Commun. 4, 2443 (2013).
[NPL 10] Yoshimaru, T. *et al.*, Sci Rep. 7(1), 1821 (2017)

[Summary]

[Technical Problem]

[0006]

As mentioned above, growth suppression actions on breast cancer cells by a dominant negative peptide of BIG 3 has been elucidated. However, the stability of the known dominant negative peptide cannot be said to be high, and the duration of inhibitory effects on the BIG3-PHB2 interaction is not that long. Then, the present inventors discovered that the duration of inhibitory effects on the BIG3-PHB2 interaction is improved by introducing a stapling structure (bridging structure) into the above-mentioned dominant negative peptide molecule (PCT/JP2017/001187, and Yoshimaru, T. *et al.*, Sci Rep. 7(1), 1821 (2017)). Peptides to which a stapling structure has been introduced (stapled peptides; stERAP No. 12 and such) were confirmed to show more stable effects of suppressing breast cancer growth.

The above-mentioned stapled peptides prolonged the duration of the inhibitory effects

on the BIG3-PHB2 interaction. However, inhibitory effects that last even longer are desired for clinical applications.

[0007]

Therefore, an objective of the present disclosure is to provide peptides having longer lasting inhibitory effects on the BIG3-PHB2 interaction.

[Solution to Problem]

[0007a]

In one aspect, the present disclosure provides a peptide comprising an amino acid sequence in which at least two pairs of amino acid residues are substituted with the same number of stapling structures in the amino acid sequence of SEQ ID NO: 4 or SEQ ID NO: 5, or a salt thereof, wherein the two pairs of amino acid residues are either (a) and (b), or (c) and (d) below: (a) the third and seventh amino acid residues from the N terminus of the amino acid sequence of SEQ ID NO: 4; and (b) the eighth and twelfth amino acid residues from the N terminus of the amino acid sequence of SEQ ID NO: 4, or (c) the third and seventh amino acid residues from the N terminus of the amino acid sequence of SEQ ID NO: 5; and (d) the tenth and fourteenth amino acid residues from the N terminus of the amino acid sequence of SEQ ID NO: 5.

[0007b]

In one aspect, the present disclosure provides a peptide which is a retro-inverso form of a peptide comprising an amino acid sequence in which at least two pairs of amino acid residues are substituted with the same number of stapling structures in the amino acid sequence of SEQ ID NO: 4 or SEQ ID NO: 5, or a salt thereof, wherein the two pairs of amino acid residues are (a) and (b) below: (a) the third and seventh amino acid residues from the N terminus of the amino acid sequence of SEQ ID NO: 4; and (b) the eighth and twelfth amino acid residues from the N terminus of the amino acid sequence of SEQ ID NO: 4, or wherein the two pairs of amino acid residues are (c) and (d) below: (c) the third and seventh amino acid residues from the N terminus of the amino acid sequence of SEQ ID NO: 5; and
(d) the tenth and fourteenth amino acid residues from the N terminus of the amino acid sequence of SEQ ID NO: 5.

[0007c]

In another aspect, the present disclosure provides a pharmaceutical composition comprising the peptide or the salt thereof as described herein and a pharmaceutically acceptable carrier.

[0007d]

In another aspect, the present disclosure provides use of the pharmaceutical composition as described herein in the manufacture of a medicament for treating cancer.

[0008]

The present inventors previously discovered that the duration of inhibitory effects on the BIG3-PHB2 interaction is improved by introducing a stapling structure into the above-mentioned dominant negative peptide molecule, and now the present inventors completed the present disclosure by discovering that stability is enhanced by further increasing the number of intramolecular crosslinks. More specifically, the present disclosure provides the following peptides and uses thereof:

[0009]

[1] a peptide comprising an amino acid sequence in which at least two pairs of amino acid residues are substituted with the same number of stapling structures in the amino acid sequence of SEQ ID NO: 4 or SEQ ID NO: 5, or a salt thereof;

[2] the peptide or the salt thereof of [1], wherein two pairs of amino acid residues are substituted with two stapling structures;

[3] the peptide or the salt thereof of [1] or [2], wherein the two pairs of amino acid residues are (a) and (b) below:

(a) the third and seventh amino acid residues from the N terminus of the amino acid sequence of SEQ ID NO: 4; and

(b) the eighth and twelfth amino acid residues from the N terminus of the amino acid sequence of SEQ ID NO: 4;

[4] the peptide or the salt thereof of [1] or [2], wherein the two pairs of amino acid residues are (c) and (d) below:

(c) the third and seventh amino acid residues from the N terminus of the amino acid sequence of SEQ ID NO: 5; and

(d) the tenth and fourteenth amino acid residues from the N terminus of the amino acid sequence of SEQ ID NO: 5;

[5] the peptide or the salt thereof of any one of [1] to [4], wherein the stapling structure is represented by Formula (I) below:

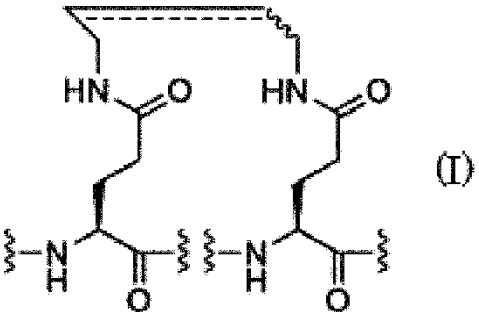

(I)

(wherein, the double line drawn by a solid line and a dashed line indicates a single bond or a double bond);

[6] the peptide or the salt thereof of [5], wherein the stapling structure is represented by Formula (II) below:

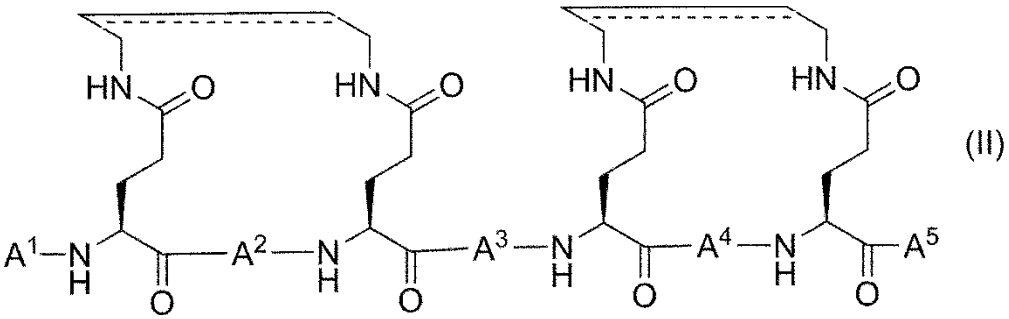

(II)

(wherein, the double line drawn by a solid line and a dashed line indicates a single bond or a double bond;

the combination of A^1, A^2, A^3, A^4, and A^5 is selected from the following:

A^1 = QM, A^2 = SDL, A^3 = –, A^4 = QLR, and A^5 = R; and

A^1 = QM, A^2 = SDL, A^3 = LQ, A^4 = RQR, and A^5 = OH;

wherein "–" indicates a peptide bond with no additional amino acid residue (that is, two stapling structures are connected); and "OH" indicates that one end of the above stapling structure constitutes the C terminus of the peptide derivative);

[7] the peptide or the salt thereof of any one of [1] to [6], wherein either one or both of N-terminal and C-terminal amino acid residues have been modified;

[8] the peptide or the salt thereof of [7], wherein either one or both of N-terminal and C-terminal amino acid residues have been modified by any one or a combination of acetylation, amidation, and HA tagging;

[9] the peptide or the salt thereof of [8], wherein the N-terminal amino acid residue is acetylated and the C-terminal amino acid residue is amidated;

[10] the peptide or the salt thereof of any one of [1] to [9], wherein all the amino acid residues have been substituted with D-form amino acid residues;

[11] a peptide which is a retro-inverso form of the peptide of any one of [1] to [9], or a salt

thereof;
[12] a pharmaceutical composition comprising the peptide or the salt thereof of any one of [1] to [11] and a pharmaceutically acceptable carrier;
[13] the pharmaceutical composition of [12], which is for cancer therapy;
[14] the pharmaceutical composition of [13], wherein the cancer is breast cancer or prostate cancer; and
[15] the pharmaceutical composition of [13] or [14], wherein the cancer is estrogen receptor-positive cancer.
[0010]

Alternatively, the present invention provides a method for cancer therapy, which comprises the step of administering the peptide or the salt thereof of any one of the above-mentioned [1] to [11] to a subject in need of the therapy. Furthermore, the present invention relates to use of the peptide or the salt thereof of any one of the above-mentioned [1] to [11] in the production of pharmaceutical compositions for cancer therapy. The present invention also relates to use of the peptide or the salt thereof of any one of the above-mentioned [1] to [11] in cancer therapy. Additionally, the present invention relates to a method of producing a pharmaceutical composition for cancer therapy, which comprises the step of mixing or formulating the peptide or the salt thereof of any one of the above-mentioned [1] to [11] with a carrier.

[Effects of the Invention]
[0011]

Peptides having longer lasting inhibitory effects on the BIG3-PHB2 interaction are provided by the present invention. Pharmaceutical compositions comprising a peptide of the present invention may be applied to cancer therapy.

[Brief Description of Drawings]
[0012]
[Fig. 1]

Fig. 1 shows schematic diagrams of double stapled ERAPs (No. 45 and No. 46).
[Fig. 2]

Fig. 2 shows that double stapled ERAPs suppress the growth of an estrogen-dependent human breast cancer cell line stably for a long time. (Figs. 2A and B) Human breast cancer cell line MCF-7 cells were treated with double stapled ERAP No. 45 (A) or double stapled ERAP No. 46 (B). Immediately thereafter, the cells were stimulated with 10 nM estrogen, and inhibitory effects were evaluated every 24 hours up to 96 hours by the MTT assay. Data

represent the mean ± standard deviation of three independent experiments. (C) Sigmoidal curves for the peptide concentrations (0.01, 0.05, 0.1, 0.5, 1, 5, and 10 μM) of single stapled ERAP (filled circle), double stapled ERAP No. 45 (filled triangle), or double stapled ERAP No. 46 (filled square), *versus* the percentage of growth suppression are shown.

[Fig. 3]

Fig. 3 shows the chymotrypsin resistance of double stapled ERAPs. The chromatograms for double stapled ERAP No. 45 (A) and double stapled ERAP No. 46 (B), when a double stapled ERAP was reacted with chymotrypsin at 37°C for 24 hours, are shown. In the experiment, the double stapled ERAP-chymotrypsin reaction solutions were subjected to high performance liquid chromatography (reverse-phase column, 0.3 mL/min flow rate, gradient elution (solution A: 0.1% trifluoroacetic acid; solution B: 0.1% trifluoroacetic acid/acetonitrile, A/B = 90/10 (0-20 min) to 40/60 (20-80 min))), and detection was carried out by UV at 210 nm.

[Fig. 4]

Fig. 4 shows the results of MTT assay which indicate that double stapled ERAP No. 46 has no effect against the growth of mammary epithelial cell line MCF-10A. MCF-10A cells were treated with the double stapled ERAP at the concentrations shown in the drawing up to 96 hours, and cell growth was evaluated every 24 hours.

[Fig. 5]

Fig. 5 shows that double stapled ERAP No. 46 inhibits the interaction between BIG3 and PHB2. (A, B) Inhibitory effect of double stapled ERAP No. 46 on BIG3-PHB2 interaction in MCF-7 cells was evaluated by Western blotting. MCF-7 cells were treated with double stapled ERAP No. 46 and single stapled ERAP at 1 μM and 10 μM, and immediately thereafter, stimulated using 10 nM estrogen for 24 hours (A) and for 96 hours (B). Then, the cells were lysed, immunoprecipitation was performed using an anti-BIG3 antibody, and immunoblot analyses were performed using the antibodies indicated in the drawing. The binding inhibition rates are expressed as proportions to the band area for PHB2 in untreated cells which is set as 100.

[Fig. 6]

Figs. 6 to 8 show the schemes for synthesis of a stapled ERAP. Fig. 6 shows a scheme for synthesis of an amino acid derivative used for the synthesis of stapled ERAPs. (i) to (vi) indicate reagents and amino acid synthesis conditions for each of the reactions: (i) 2,4-dimethoxybenzaldehyde, AcOH, $MgSO_4$, CH_2Cl_2; (ii) $NaBH_4$, MeOH, CH_2Cl_2, 87% yield (two steps); (iii) Compound 2, EDC·HCl, DIPEA, CH_2Cl_2, 76% yield; (iv) $LiOH·H_2O$, THF, MeOH, H_2O, 92% yield; (v) TBSOTf, 2,6-lutidine, CH_2Cl_2; (vi) Fmoc-OSu, Na_2CO_3, THF, H_2O, 90% yield (two steps).

[Fig. 7]

Fig. 7 shows a scheme for stapling synthesis on ERAP by ring-closing olefin metathesis.

[Fig. 8]

Fig. 8 shows a scheme for stapling synthesis on ERAP through intramolecular amidation.

[Fig. 9]

Fig. 9 shows that binding of PI3K occurs estrogen independently in an ESR1 mutant breast cancer cell line.

(A) Immunoblots are shown which indicate that ERα binds with PI3K in the presence of estrogen in a breast cancer cell line carrying a wild-type ESR1. MCF-7 cells were transfected with FLAG-tagged ESR1 (WT), cell lysate thereof was subjected to immunoprecipitation using an anti-FLAG antibody, and immunoblot analyses were performed using the antibodies indicated in the drawing. (B) Immunoblots are shown which analyzed the phosphorylation of PI3K, PKCα, and PHB2 when MCF-7 cells transfected with the Y537S mutant ESR1 were treated with 10 μM stERAP. MCF-7 cells were transfected with the FLAG-tagged ESR1 mutant (Y537S), lysates of cells treated with 10 μM stERAP for various lengths of time were immunoprecipitated using an anti-ERα antibody, and immunoblot analyses were performed using the antibodies indicated in the drawing.

[Fig. 10-1]

Fig. 10 shows that ESR1 mutant breast cancer cell lines have estrogen-independent high PKCα activity. (A) The PKCα activities of breast cancer cell lines transfected with an ESR1 mutant are shown. HEK293T cells and MCF-7 cells transfected with each ESR1 mutant were treated for 24 hours with PKCα inhibitor staurosporine and then subjected to immunoprecipitation using an anti-PKCα antibody, and PKCα activities were measured using the PHB2 peptide carrying Ser39 (YGVRESVFTVE (SEQ ID NO: 17)) as the substrate. The immunoprecipitates of PKCα were subjected to immunoblot analyses using the antibody indicated in the drawing. Data represent the mean ± standard error of three independent experiments (*** $P < 0.001$).

[Fig. 10-2]

(B) It was shown that the PKCα activity of a breast cancer cell line transfected with an ESR1 mutant is PI3K-dependent. MCF-7 cells transfected with each ESR1 mutant were treated for 24 hours with PI3K inhibitor wortmannin at 100 nM and then subjected to immunoprecipitation using an anti-PKCα antibody, and PKCα activities on the PHB2 peptide carrying Ser39 were measured. Data represent the mean ± standard error of three independent experiments (NS: no statistical significance; *** $P < 0.001$). (C) Immunoblots are shown which indicate that the phosphorylated PKCα of MCF-7 cells transfected with an ESR1 mutant is PI3K-dependent. MCF-7 cells transfected with each ESR1 mutant were treated for 24 hours

with stERAP and wortmannin and then subjected to immunoprecipitation using an anti-PKCα antibody, and immunoblot analyses were performed using the antibodies indicated in the drawing.

[Fig. 11-1]

Fig. 11 shows the inhibitory effects by combined use of stERAP and an anti-estrogen agent against the growth of MCF-7 cells transfected with an ESR1 mutant. MCF-7 cells transfected with each ESR1 mutant were reacted for 96 hours with 10 μM stERAP and 1 μM of tamoxifen (TAM) and 2 μM of fulvestrant (Fluv) which are anti-estrogen agents and 0.5 μM of everolimus (Ever) which is an mTOR inhibitor. Then, the cell growth was evaluated. Data represent the mean ± standard error of three independent experiments (* $P < 0.05$, ** $P < 0.01$, and *** $P < 0.001$).

[Fig. 11-2]

Fig. 11-2 is the continuation of Fig. 11-1.

[Fig. 12]

Fig. 12 shows the inhibitory effects of stERAP on growth of MCF-7 cells transfected with an ESR1 mutant in the presence of estrogen. MCF-7 cells transfected with each ESR1 mutant were reacted for 24 hours with 10 μM stERAP in the presence of estrogen at various concentrations (0.1 nM, 1 nM, or 10 nM), and the cell growth was evaluated. Data represent the mean ± standard error of three independent experiments (* $P < 0.05$, ** $P < 0.01$, and *** $P < 0.001$).

[Fig. 13]

Fig. 13 shows the inhibitory effects of stERAP on ERα transcriptional activity in the presence of estrogen in MCF-7 cells transfected with an ESR1 mutant. MCF-7 cells transfected with each ESR1 mutant were reacted for 24 hours with 10 μM stERAP in the presence of estrogen at various concentrations (0.1 nM, 1 nM, or 10 nM), and ERE-luciferase activities (ERα transcription activities) were measured. Data represent the mean ± standard error of three independent experiments.

[Fig. 14]

In Fig. 14, cell growth was evaluated for ESR1 Y537S knocked-in MCF-7 cells, when the cells were reacted for 24 hours with stERAP alone at various concentrations shown in the drawing (horizontal axis) and in the presence of 10 nM estrogen. Data represent the mean ± standard error of three independent experiments.

[Fig. 15]

Fig. 15 shows that BIG3 in a HER2-positive breast cancer cell line functions as AKAP. (A) The expression of BIG3 in a HER2-positive breast cancer cell line is shown. The mRNA levels of BIG3 in a luminal type breast cancer cell line (MCF-7 cells), HER2-positive breast

cancer cell lines (BT-474 cells, SK-BR-3 cells, and KPL-4 cells), and a normal mammary gland cell line (MCF-10A cells) were determined by real-time PCR. Data were normalized by the β2-MG content and expressed as multiples (-fold) of the value in MCF-10A cells, with that value being defined as 1.0. Data represent the mean ± standard error of three independent experiments. (B) Immunoblots are shown which indicate that BIG3 binds with PKA, PP1Cα, and PHB2. SK-BR-3 cells and KPL-4 cells were lysed, the cell lysates were immunoprecipitated using an anti-BIG3 antibody and a rat IgG antibody, and immunoblot analyses were performed using the antibodies shown in the drawing. Data shown are representatives from three independent experiments. (C) The kinase activity and phosphatase activity of BIG3 are shown. SK-BR-3 cells were treated for 24 hours with 10 μM H-89, 100 μg/mL trastuzumab, and 10 nM lapatinib, cell lysates thereof were subjected to immunoprecipitation using an anti-BIG3 antibody, and their PKA activity and PP1Cα activity were calculated using CREBtide and p-NPB as substrates. SK-BR3 cell lysate was subjected to immunoprecipitation using a rat anti-IgG antibody, and this was used as a negative control. Data represent the mean ± SE of three independent experiments (*** $P < 0.001$).

[Fig. 16]

Fig. 16 shows the mechanism for activation of BIG3 in a HER2-positive breast cancer cell line. Immunoblots are shown which indicate that BIG3 is phosphorylated by PKA through HER2 signaling. SK-BR-3 cells and KPL-4 cells were treated for 30 minutes with 10 μM H-89, 100 μg/mL trastuzumab, and 10 nM lapatinib, cell lysates thereof were subjected to immunoprecipitation using an anti-BIG3 antibody, and immunoblot analyses were performed using the antibodies shown in the drawing.

[Fig. 17]

Fig. 17 shows that BIG3 controls the suppressive activity of PHB2 in a HER2-positive breast cancer cell line. (A) Immunoblots are shown which indicate that BIG3 binds to PHB2 and controls its phosphorylation. SK-BR-3 cells and KPL-4 cells were treated for 24 hours with 1 μM stERAP, cell lysates thereof were subjected to immunoprecipitation using an anti-BIG3 antibody and an anti-PHB2 antibody, and immunoblot analyses were performed using the antibodies shown in the drawing. (B) Immunoblots are shown which indicate that PHB2 is phosphorylated *via* EGFR signaling at Ser39. After suppressing PKA expression by the siRNA method, SK-BR-3 cells were treated for 24 hours with 1 μM stERAP and SK-BR-3 cells were treated with 100 μg/mL trastuzumab and 10 nM lapatinib in the presence of 1 μM stERAP. Cells were lysed respectively and were immunoprecipitated using an anti-PHB2 antibody, and immunoblot analyses were performed using the antibodies shown in the drawing.

[Fig. 18]

Fig. 18 shows PKCα-dependent phosphorylation of PHB2 (Ser39). (A) Immunoblots

are shown which indicate that PHB2 (Ser39) is phosphorylated in a PKCα-dependent manner in a HER2-positive breast cancer cell line. SK-BR-3 cells in which PKCα expression was suppressed by the siRNA method were treated for 24 hours with 1 μM stERAP, then cell lysate thereof was subjected to immunoprecipitation using an anti-PHB2 antibody, and immunoblot analyses were performed using the antibodies shown in the drawing. (B) PKCα activity by EGFR signaling in SK-BR-3 cells is shown. SK-BR-3 cells were treated for 24 hours with 1 μM stERAP, and with 10 nM lapatinib in the presence of stERAP, cell lysates thereof were subjected to immunoprecipitation using an anti-PKCα antibody, and PKCα activities were calculated using CREBtide as a substrate. Data represent the mean ± standard error of three independent experiments.

[Fig. 19]

Fig. 19 shows that phosphorylated PHB2 (Ser39) suppresses transcriptional activity in the nucleus. (A) Immunoblots are shown which indicate that transcriptional repressors NcoR and HDAC1 bind to phosphorylated PHB2 (Ser39). SK-BR-3 cells in which PHB2 expression was suppressed by the siRNA method were transfected with the HA-tagged PHB2 construct (WT), the alanine mutant at Ser39 (S39A), and the glutamic acid mutant at Ser39 (S39E), and 48 hours later, these were treated for 24 hours with 1 μM stERAP. The nuclear fractions were isolated by specific gravity centrifugation, then the nuclear extract solutions were subjected to immunoprecipitation using an anti-HA antibody, and immunoblot analyses were performed using the antibodies shown in the drawing. (B) Immunoblots are shown which indicate that phosphorylation of PHB2 (Ser39) could not suppress HER2 signaling. SK-BR-3 cells were treated for 24 hours with 100 μg/mL trastuzumab and 10 nM lapatinib in the presence of 1 μM stERAP, cell lysates thereof were subjected to immunoprecipitation using an anti-HER2 antibody, and immunoblot analyses were performed using the antibodies shown in the drawing.

[Fig. 20]

Fig. 20 shows the threonine phosphorylation in PHB2 and activation mechanism therefor. (A) Immunoblots are shown which indicate that threonine phosphorylation of PHB2 is induced PKCα-independently in a HER2-positive breast cancer cell line. SK-BR-3 cells in which PKCα expression was suppressed by the siRNA method were treated for 24 hours with 1 μM stERAP and 100 μg/mL trastuzumab, then cell lysates thereof were subjected to immunoprecipitation using an anti-PHB2 antibody, and immunoblot analyses were performed using the antibodies shown in the drawing. (B) Immunoblots are shown which indicate that PHB2 is threonine phosphorylated by TTK and MK5. SK-BR-3 cells in which TTK, CHK1, and MK5 expressions were suppressed by the siRNA method were treated for 24 hours with 1 μM stERAP, then the cells were lysed and subjected to immunoblot analyses using the antibodies shown in the drawing.

[Fig. 21]

Fig. 21 shows the effects of threonine phosphorylation of PHB2 caused by TTK and MK5, on the HER2 signal. (A, B) Immunoblots are shown which indicate that threonine phosphorylation of PHB2 caused by TTK and MK5 inhibits the HER2-HER3 binding and HER2-Shc binding. SK-BR-3 cells (A) and KPL-4 cells (B) in which TTK, MK5, and CHK1 expressions were suppressed by the siRNA method were treated for 24 hours with 1 μM stERAP, then the cells were lysed and subjected to immunoprecipitation using an anti-HER2 antibody, and immunoblot analyses were performed using the antibodies shown in the drawing. (C) Immunoblots are shown which indicate that inhibition of HER2-HER3 binding and HER2-Shc binding by PHB2 is avoided by a TTK inhibitor. SK-BR-3 cells were treated for 24 hours with 2 μM AZ3146 and 1 μM stERAP, and then cell lysates thereof were subjected to immunoprecipitation using an anti-HER2 antibody, and immunoblot analyses were performed using the antibodies shown in the drawing.

[Fig. 22]

Fig. 22 shows identification of the threonine phosphorylation sites in PHB2. (A) Immunoblots are shown which evaluate Thr42 and Thr169 as the threonine phosphorylation sites in PHB2. SK-BR-3 cells in which PHB2 expression was suppressed by the siRNA method were transfected with the HA-tagged PHB2 construct, alanine mutant at Thr42 (T42A), alanine mutant at Thr169 (T169A), and double alanine mutant at Thr42 and Thr169 (T42A+T169A). 48 hours later, these were treated for 24 hours with 1 μM stERAP. The cells were then lysed and subjected to immunoprecipitation using an anti-HA antibody, and immunoblot analyses were performed using the antibodies shown in the drawing. (B) Immunoblots are shown which indicate that phosphorylation of Thr42 and Thr169 in PHB2 inhibits HER2-HER3 binding and HER2-Shc binding. SK-BR-3 cells in which PHB2 expression was suppressed by the siRNA method were transfected with the HA-tagged PHB2 construct, alanine mutant at Thr42 (T42A), alanine mutant at Thr169 (T169A), and double alanine mutant at Thr42 and Thr169 (T42A+T169A). 48 hours later, these were treated for 24 hours with 1 μM stERAP. The cells were then lysed and subjected to immunoprecipitation using an anti-HER2 antibody and an anti-BIG3 antibody, and immunoblot analyses were performed using the antibodies shown in the drawing.

[Fig. 23]

Fig. 23 shows threonine phosphorylation of PHB2 caused by TTK and MK5. (A) Immunoblots are shown which indicate that PHB2 binds to TTK. SK-BR-3 cells were treated for 24 hours with 1 μM stERAP, then the cells were lysed and subjected to immunoprecipitation using an anti-PHB2 antibody, an anti-TTK antibody, and a rabbit IgG antibody, and immunoblot analyses were performed using the antibodies shown in the drawing. (B, C) Immunoblots are

shown which used Phos-tag to evaluate threonine phosphorylation of PHB2 by TTK and MK5. Recombinant TTK (B) and recombinant MK5 (C) were reacted with recombinant PHB2 at varied molar ratios with respect to PHB2 at 30°C for 30 minutes in the presence of ATP. Thereafter, immunoblot analyses by Phos-tag were performed using the antibodies shown in the drawing.

[Fig. 24]

Fig. 24 shows the suppressive effects of stERAP on the growth of HER2-positive breast cancer cell lines. The results of MTT assays evaluating the inhibitory effects of stERAP on the growth of HER2-positive breast cancer cell lines are shown. SK-BR-3 cells, BT-474 cells, and KPL-4 cells were reacted with stERAP for 24 hours. Data represent the mean ± SE of three independent experiments (* $P < 0.05$, ** $P < 0.01$, and *** $P < 0.001$).

[Fig. 25]

Fig. 25 shows that stERAP inhibits HER2-HER3 interaction and HER2-Shc interaction. Immunoblots are shown which indicate that stERAP inhibits HER2-HER3 interaction and HER2-Shc interaction in HER2-positive breast cancer cell lines. HER2-positive breast cancer cell lines (SK-BR-3 cells, BT-474 cells, and KPL-4 cells) were treated for 24 hours with stERAP at various concentrations and 100 μg/mL trastuzumab, then cell lysates thereof were subjected to immunoprecipitation using an anti-HER2 antibody, and immunoblot analyses were performed using the antibodies shown in the drawing.

[Fig. 26]

Fig. 26 shows the suppressive effects of stERAP on trastuzumab-resistant HER2-positive breast cancer cell lines. (A) The results of MTT assays are shown, which evaluated the inhibitory effects of stERAP on the growth of trastuzumab-resistant HER2-positive breast cancer cell lines. Trastuzumab-resistant SK-BR-3 cells were reacted for 24 hours with stERAP and trastuzumab. Data represent the mean ± SE of three independent experiments (* $P < 0.05$, ** $P < 0.01$, and *** $P < 0.001$). (B) Immunoblots are shown which indicate that stERAP inhibits HER2-HER3 interaction and HER2-Shc interaction in a trastuzumab-resistant HER2-positive breast cancer cell line. SK-BR-3 cells and trastuzumab-resistant SK-BR-3 cells were treated for 24 hours with 20 μM stERAP and 100 μg/mL trastuzumab, then cell lysates thereof were subjected to immunoprecipitation using an anti-HER2 antibody, and immunoblot analyses were performed using the antibodies shown in the drawing.

[Fig. 27]

Fig. 27 shows the effects of stERAP on NF-κB signal in trastuzumab-resistant HER2-positive breast cancer cell lines. Immunoblots are shown which indicate that stERAP suppresses nuclear translocation of NF-κB and phosphorylation of IκBα in a trastuzumab-resistant HER2-positive breast cancer cell line. SK-BR-3 cells and trastuzumab-resistant SK-

BR-3 cells were treated for 24 hours with 20 μM stERAP and 100 μg/mL trastuzumab, then the cells were lysed, and immunoblot analyses were performed using the antibodies shown in the drawing.

[Fig. 28]

Fig. 28 shows the effects of stERAP on the cell cycle of trastuzumab-resistant HER2-positive breast cancer cell lines. FACS analyses showing the effects of stERAP on the cell cycle are shown. Trastuzumab-resistant SK-BR-3 cells were treated for 24 hours with 20 μM stERAP and 100 μg/mL trastuzumab, then the cells were fixed, stained by propidium iodide, and analyzed by flow cytometry.

[Fig. 29]

Fig. 29 shows the *in vivo* antitumor effects of stERAP on trastuzumab-resistant HER2-positive breast cancer cells. The inhibitory effects of stERAP on tumor growth in mouse models subjected to orthotopic transplantation of KPL-4 cells and trastuzumab-resistant SK-BR-3 cells are shown. The left panel shows the change in tumor diameter in the group receiving administration of 150 μg/kg of stERAP every seven days, and the right panel shows the change in mouse body weight. Each symbol in each graph indicates the following: filled circle: untreated; and open circle: 150 μg/kg stERAP. Data on tumor diameter and body weight represent the mean ± standard error of each group ($n = 5$, $^{***}P < 0.001$).

[Fig. 30]

Fig. 30 shows the results of investigating the effects of three types of stERAP (single stERAP, double stERAP #45, and double stERAP #46) on cell growth of three types of breast cancer cell lines (SK-BR-3, BT-20, and MDA-MB-231) and synovial sarcoma cell line SW982. For the single stERAP and double stERAP #46, peptides were added at a total of eleven concentrations prepared by three-fold serial dilution starting from 20 μM. For the double stERAP #45, peptides were added at a total of eight concentrations prepared by two-fold serial dilution starting from 50 μM. The number of viable cells were measured 96 hours after the peptide addition, and relative values thereof were calculated based on the negative control cells without peptide addition and plotted. Experiments using double stERAP #45 on the SW982 cell line were not carried out.

[Fig. 31-1]

Fig. 31 shows the results of investigating the effects of two types of stERAPs (single stERAP and double stERAP #46) on the cell cycle of SK-BR-3 cells (Fig. 31A) and MDA-MB-231 cells (Fig. 31B). Each peptide was added at 5 μM concentration. 96 hours later, the cells were stained with Propidium Iodide (PI). Fluorescence intensity of each cell was measured using a flow-cytometer and histograms were prepared. In the graphs, the percentages of the number of cells at each phase of the cell cycle (Sub G1 phase, G1 phase, S phase, and G2/M

phase; > 2 N cells) are shown.

[Fig. 31-2]

Fig. 31-2 is the continuation of Fig. 31-1.

[Description of Embodiments]

[0013]

Although any methods and materials similar or equivalent to those described herein can be used in the practice or testing of embodiments of the present invention, the preferred methods, devices, and materials are now described. However, before the present materials and methods are described, it is to be understood that the present invention is not limited to the particular sizes, shapes, dimensions, materials, methodologies, protocols, *etc.* described herein, as these may vary in accordance with routine experimentation and optimization. It is also to be understood that the terminology used in the description is for the purpose of describing the particular versions or embodiments only, and is not intended to limit the scope of the present invention which will be limited only by the appended claims.

[0014]

Definitions

The words “a”, “an”, and “the” used herein mean “at least one” unless otherwise specifically indicated.

[0015]

Herein, unless otherwise specifically indicated, amino acids represented by capital letters indicate L-amino acids. Amino acids represented by lower-case letters indicate D-amino acids. Furthermore, L-amino acids and D-amino acids represented herein may include amino acids in which any of amino group, carboxyl group, and side chains has been modified. Examples of preferred modifications include acetylation of the amino group, amidation of the carboxyl group, tag peptide addition such as FLAG-tagging and HA-tagging, and such.

[0016]

Herein, numbers indicating the positions of amino acid residues in amino acid sequences have been given with the N-terminal amino acid residue as number 1 and in order toward the C terminus, unless otherwise specifically indicated.

[0017]

The term “BIG3” used herein refers to brefeldin A-inhibited guanine nucleotide-exchange protein 3. BIG3 forms a complex with PHB2 to inhibit the estrogen-dependent transcriptional activation-suppressing function of PHB2. BIG3 is also referred to as “ARFGEF family member 3 (ARFGEF3)” or “A7322”. An example of a representative nucleotide sequence of the human BIG3 gene is shown in SEQ ID NO: 6 (GenBank Accession No.

NM_020340.4), and the amino acid sequence encoded by the gene is shown in SEQ ID NO: 7. In the present invention, BIG3 is not limited to that encoded by the aforementioned nucleotide sequence and also encompasses their isoforms and mutants.

[0018]

The term "PHB2" used herein refers to prohibitin 2. PHB2 binds to estrogen receptors to inhibit estrogen receptor signaling pathways and suppresses estrogen-dependent cell growth. PHB2 is also referred to as "Repressor of Estrogen Activity (REA)". Examples of representative nucleotide sequences of the human PHB2 gene are shown in SEQ ID NO: 8 (GenBank Accession No. NM_001144831.1) and SEQ ID NO: 10 (GenBank Accession No. NM_001267700.1), and the amino acid sequences encoded by the genes are shown in SEQ ID NO: 9 and SEQ ID NO: 11, respectively. In the present invention, PHB2s are not limited to those encoded by the aforementioned nucleotide sequences and also encompass their isoforms and mutants.

[0019]

The term "PHB2 peptide" used herein refers to a PHB2-derived peptide which inhibits the binding between BIG3 and PHB2. Specifically, it includes the amino acid sequence (YGVRESVFTVE) shown in SEQ ID NO: 17.

[0020]

The term "estrogen receptor" used herein encompasses both estrogen receptor α (ERα) and estrogen receptor β (ERβ). Estrogen receptors translocate into the nucleus when bound by estrogen, and bind to the enhancer sequence ERE on a DNA to cause transcriptional activation of genes relating to cell growth. This induces estrogen-dependent cell growth. ERα and ERβ are encoded by the ESR1 gene and ESR2 gene, respectively. The nucleotide sequence of a representative human ESR1 gene is shown in SEQ ID NO: 12 (GenBank Accession No. NM_000125.3). Furthermore, the nucleotide sequence of a representative human ESR2 gene is shown in SEQ ID NO: 14 (GenBank Accession No. NM_001437.2). In the present invention, ERα and ERβ are not limited to those encoded by the aforementioned nucleotide sequences and also encompass their isoforms and mutants. In a preferred embodiment of the present invention, the estrogen receptor is ERα.

[0021]

The term "ERAP" used herein refers to a peptide consisting of the amino acid sequence of SEQ ID NO: 4 or SEQ ID NO: 5. The amino acid sequence of SEQ ID NO: 4 or SEQ ID NO: 5 is a sequence consisting of the 165th to 177th amino acid residues or the 165th to 178th amino acid residues in the amino acid sequence of BIG3 (SEQ ID NO: 7), and contains amino acid residues important for binding with PHB2 (glutamine (Q) at position 165, aspartic acid (D) at position 169, and glutamine (Q) at position 173 in the amino acid sequence of SEQ ID NO: 7).

ERAP has an ability to bind to PHB2 and inhibits BIG3 from forming the complex with PHB2 by binding competitively to PHB2.

[0022]

The term “stapling structure” used herein refers to a structure in which two (a pair of) amino acid residues in an amino acid sequence constituting a peptide are crosslinked. Herein, a peptide in which original amino acid residues are substituted with one or a plurality of stapling structures is referred to as “a stapled peptide”. For example, a stapled ERAP (stERAP or stapled ERAP) is a peptide in which at least one pair of amino acid residues in the peptide consisting of the amino acid sequence of SEQ ID NO: 4 or SEQ ID NO: 5 (ERAP) has been substituted with a stapling structure. A short stapled ERAP refers to a peptide in which at least one pair of amino acid residues in a peptide consisting of a partial sequence of the amino acid sequence of SEQ ID NO: 4 or SEQ ID NO: 5 (short ERAP) has been substituted with a stapling structure. Herein, a short stapled ERAP is also written as “sh stapled ERAP”.

A peptide in which the original amino acid residues are substituted with one stapling structure is referred to as a “single stapled peptide” or a “single crosslinked peptide”, and a peptide in which the original amino acid residues are substituted with two stapling structures is referred to as a “double stapled peptide” or a “double crosslinked peptide”. For example, a single stapled ERAP (single stERAP, or single stapled ERAP) is a peptide in which one pair of amino acid residues in the peptide consisting of the amino acid sequence of SEQ ID NO: 4 or SEQ ID NO: 5 (ERAP) has been substituted with a stapling structure; and a double stapled ERAP (dsERAP, double stERAP, or double stapled ERAP) is a peptide in which two pairs of amino acid residues in the peptide consisting of the amino acid sequence of SEQ ID NO: 4 or SEQ ID NO: 5 (ERAP) have been substituted with stapling structures.

These stapled peptides can be referred to as peptide derivatives or peptide analogs since a part of their structures has been artificially substituted.

[0023]

The term “therapy” used herein encompasses alleviation/improvement of at least one symptom caused by a target disease, suppression of progression of the disease, suppression of enlargement of the disease site, and such. For example, “cancer therapy” includes cancer cell growth suppression, suppression of cancer progression, induction of regression/remission of cancer, alleviation/improvement of symptoms accompanying cancer, suppression of cancer metastasis, suppression of postoperative recurrence, and induction of prolonged survival time.

[0024]

<u>Peptides of the present invention</u>

A peptide of the present invention is a peptide comprising an amino acid sequence in which an n pair(s) (n is a natural number) of amino acid residues is substituted with n number of

stapling structure(s) in the amino acid sequence of SEQ ID NO: 4 or SEQ ID NO: 5. Here, n is preferably 3 or less, and more preferably 2. Therefore, in the present invention, n pair(s) of amino acid residues normally refer(s) to one to three pairs, or one or two pairs, and preferably two pairs of amino acid residues.

[0025]

In the peptides of the present invention, the amino acid residues substituted by the stapling structure are not particularly limited; however, since the first amino acid residue (glutamine (Q)), the fifth (aspartic acid (D)), and the ninth (glutamine (Q)) from the N terminus of the amino acid sequence of SEQ ID NO: 4 or SEQ ID NO: 5 are important amino acid residues for binding with PHB2, from the viewpoint of binding affinity for PHB2, they are preferably selected from amino acid residues other than glutamine (Q) at the first, aspartic acid (D) at the fifth, and glutamine (Q) at the ninth from the N terminus of the amino acid sequence of SEQ ID NO: 4 (QMLSDLTLQLRQR) or SEQ ID NO: 5 (QMLSDLTLQLRQRQ).

For example, of the amino acid residues constituting the peptide, introducing a stapling structure to the leucine residue (L) provides chymotrypsin-resistance. For example, at least two pairs of amino acid residues including at least one L selected from the group consisting of the third, sixth, eighth, and tenth in the amino acid sequence of SEQ ID NO: 4 or 5 are preferred as positions for substitution with stapling structures.

[0026]

Examples of the amino acid residues substituted by the stapling structure include the following pairs of amino acid residues:

(a) the third (L) and seventh (T) amino acid residues from the N terminus of the amino acid sequence of SEQ ID NO: 4;

(b) the eighth (L) and twelfth (Q) amino acid residues from the N terminus of the amino acid sequence of SEQ ID NO: 4;

(c) the third (L) and seventh (T) amino acid residues from the N terminus of the amino acid sequence of SEQ ID NO: 5; and

(d) the tenth (L) and fourteenth (Q) amino acid residues from the N terminus of the amino acid sequence of SEQ ID NO: 5.

[0027]

It is particularly preferred that the above-mentioned amino acid residues of (a) and (b), or (c) and (d) are substituted with stapling structures.

[0028]

In the peptides of the present invention, the stapling structures are not particularly limited. Peptide stapling techniques are known (for example, Blackwell, H. E. *et al.*, Angew. Chem., Int. Ed. 37, 3281-3284 (1994); Aihara, K. *et al.*, Tetrahedron 71, 4183-4191 (2015); and

such); therefore, these known stapling techniques can be used to form stapling structures. For example, stapling structures can be formed by synthesizing peptides through solid-phase synthesis or such by incorporating amino acid derivatives carrying a substituent such as an alkenyl group, and then performing an olefin metathesis reaction or an intramolecular amidation reaction between the substituents of the above-mentioned amino acid derivatives. Commercially available amino acid derivatives may be used as amino acid derivatives for forming the stapling structure.

[0029]

Examples of preferred stapling structures for the peptides of the present invention include structures represented by Formula (I) shown below:

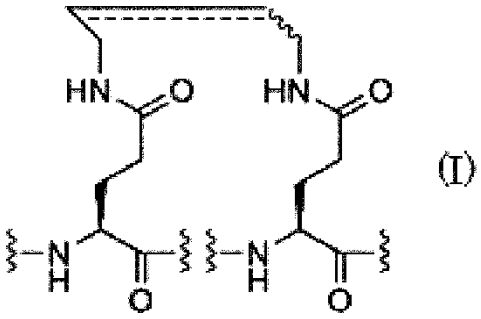

(I)

(wherein the double line drawn by a solid line and a dashed line indicates a single bond or a double bond).

[0030]

The stapling structure of Formula (I) above can be formed, for example, according to the scheme shown in Fig.7 (hereinafter, "Scheme (I)"), which is an example where the stapling structure is formed by an olefin metathesis reaction. On the other hand, the scheme shown in Fig. 8 (hereinafter "Scheme (II)") is an example where the stapling structure is formed by an intramolecular amidation reaction.

[0031]

When forming a stapling structure by the olefin metathesis reaction shown in Scheme (I), the amino acid derivative used for stapling may be the glutamine derivative (4-{allyl-[2-(*tert*-butyl-dimethyl-silanyloxy)-4-methoxy-benzyl]-carbonyl}-2-(9H-fluoren-9-yl-methoxycarbonylamino)-butyric acid) represented by Formula (III) shown below.

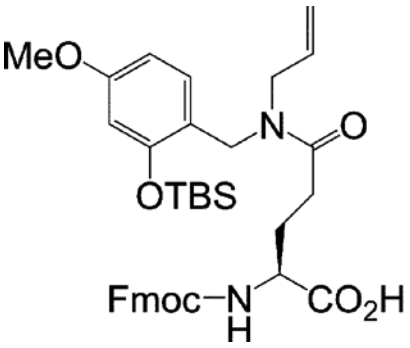

(III)

[0032]

The glutamine derivative of Formula (III) can be synthesized, for example, according to Scheme (III) shown below (Aihara, K. *et al.*, Tetrahedron 71, 4183-4191 (2015)).

[0033]

Scheme (III)

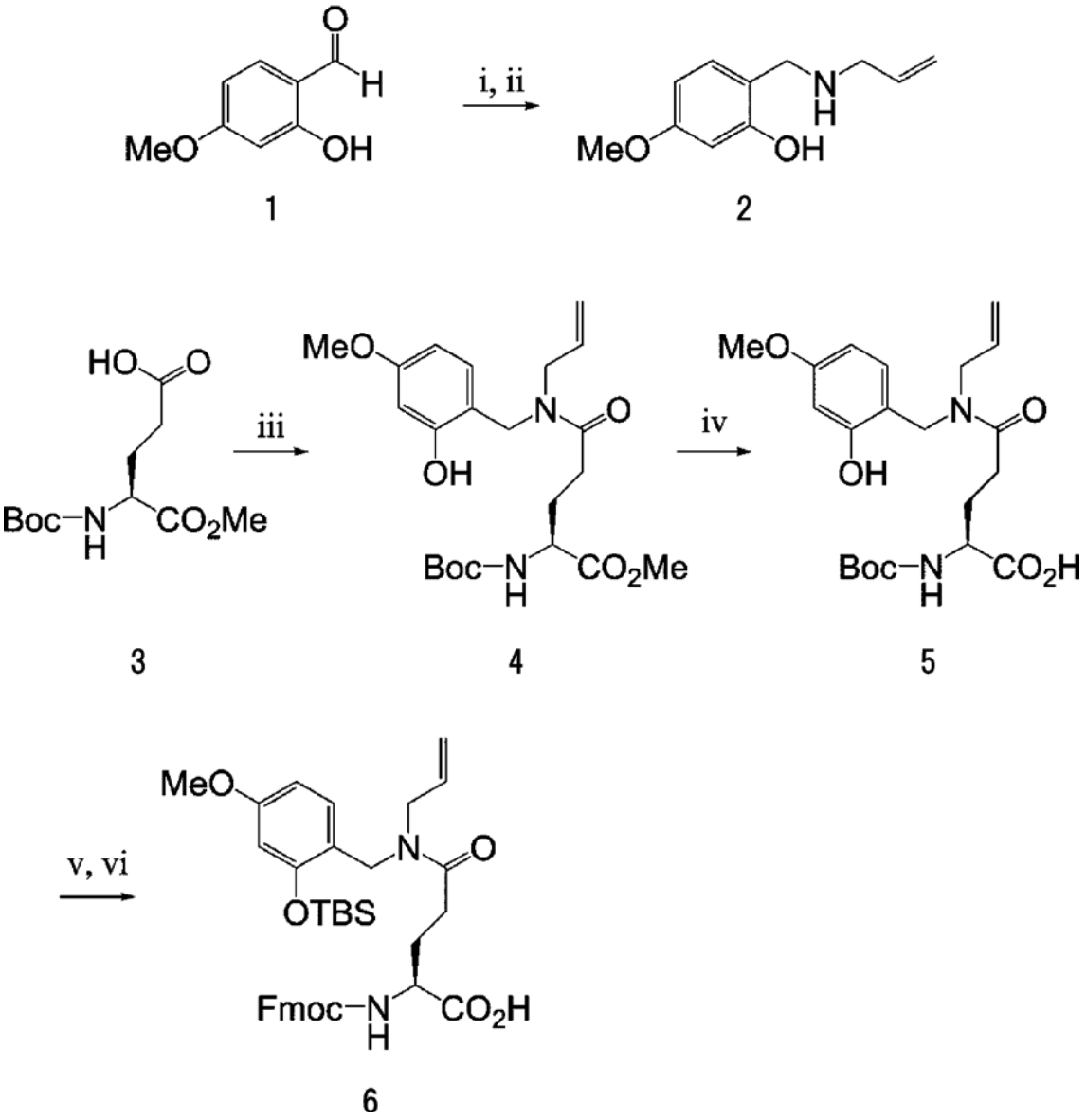

In Scheme (III) shown above, (i) to (vi) each indicate the followings: (i) 3-amino-1-propene, AcOH, $MgSO_4$, CH_2Cl_2; (ii) $NaBH_4$, MeOH, CH_2Cl_2; (iii) Compound 2, DCC, CH_2Cl_2; (iv) $LiOH \cdot H_2O$, THF, MeOH, H_2O; (v) TBSOtf, 2,6-lutidine; and (vi) Fmoc-OSu, Na_2CO_3, THF, H_2O.

[0034]

As shown in Scheme (III), 2-hydroxy-4-methoxybenzaldehyde (Compound 1) is reductively aminated with 3-amino-1-propene to obtain 2-allylaminomethyl-5-methoxy-phenol (Compound 2). Next, Compound 2 is coupled with *N*-α-(*tert*-butoxycarbonyl)-L-glutamic acid α-methyl ester (Compound 3) to obtain 4-[allyl-(2-hydroxy-4-methoxy-benzy)carbamoyl]-2-*tert*-butoxycarbonylamino-butyric acid methyl ester (Compound 4). Next, the methyl ester in Compound 4 is hydrolyzed to obtain 4-[allyl-(2-hydroxy-4-methoxy-benzyl)carbamoyl]-2-*tert*-butoxycarbonylamino-butyric acid (Compound 5). Furthermore, by substituting the Boc group of Compound 5 with an Fmoc group and protecting the phenol moiety of the Hmb group with TBS, the glutamine derivative of Formula (III) can be obtained. Commercially available reagents can be used for all the reagents necessary to carry out Scheme (III).

[0035]

On the other hand, synthesis of stapled ERAPs by Scheme (I) can be carried out using the glutamine derivative of the above-mentioned Formula (III), for example, as described below. First, a peptide is synthesized by standard Fmoc solid-phase peptide synthesis, with each amino acid residue of a pair, at a position where one wants to form a stapling structure in the amino acid sequence of SEQ ID NO: 4 or SEQ ID NO: 5, being substituted with the glutamine derivative of Formula (III). Then, after deprotection of the N terminus of the Fmoc-protected peptide followed by acetylation, the acetylated peptide is treated with Hoveyda-Grubbs' second-generation catalyst and an olefin metathesis reaction is carried out. Furthermore, deprotection of acid-labile protecting groups and cleavage of peptides from resin are performed using a cocktail of TFA/*m*-cresol/thioanisole/1,2-ethanedithiol/H_2O. Following these, stapled ERAPs or sh stapled ERAPs carrying the stapling structure of Formula (I) (the double line drawn by a solid line and a dashed line is a double bond) can be obtained. In the stapled ERAP or sh stapled ERAP synthesized by Scheme (I), the number of amino acid residues interpositioned within the stapling structure is not particularly limited, but normally the preferred number is three residues. More specifically, a structure in which a pair of amino acid residues having three residues positioned in between is substituted with a single stapling structure is a favorable example of a stapling structure in the present invention. A stapling structure having three residues positioned within it is effective for maintaining the α-helical structure of the peptide.

[0036]

Furthermore, when forming a stapling structure by the intramolecular amidation

reaction shown in Scheme (II), the amino acid derivatives used for stapling may be *N*-α-(9-fluorenylmethoxycarbonyl)-L-glutamic acid γ allyl ester represented by Formula (IV) and (S)-2-((((9H-fluoren-9-yl)methoxy)carbonyl)amino)5-((4-(((allyloxy)carbonyl)amino)butyl) (2,4-dimethoxybenzyl)amino)-5-oxopentanoic acid represented by Formula (V), shown below.

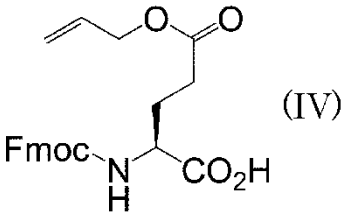

(IV)

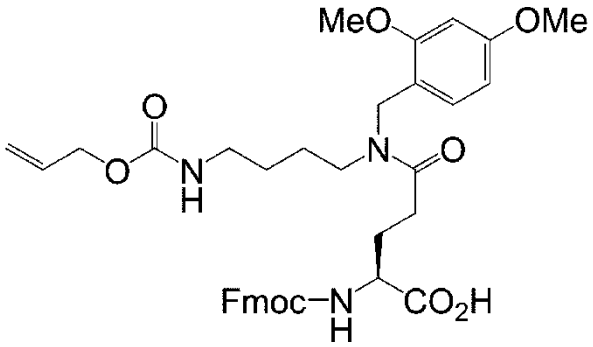

(V)

[0037]

Among the two types of amino acid derivatives described above, a commercially available product may be used for the glutamic acid derivative of Formula (IV). Furthermore, the glutamine derivative of Formula (V) can be synthesized, for example, according to the scheme shown in Fig. 6 (herein below, "Scheme (IV)"). As shown in Scheme (IV), allyl(4-aminobutyl)carbamate (Compound 1) is coupled with 2,4-dimethoxybenzaldehyde to obtain allyl[4-{(2,4-dimethoxybenzyl)amino}butyl]carbamate (Compound 2). Next, Compound 2 is coupled with *N*-α-(*tert*-butoxycarbonyl)-L-glutamic acid α methyl ester (Compound 3) to obtain (S)-methyl-5-{(4-[{(allyloxy)carbonyl}amino]butyl) (2,4-dimethoxybenzyl)amino}-2-{(*tert*-butoxycarbonyl)amino}-5-oxopentanoate (Compound 4). Next, the methyl ester in Compound 4 is hydrolyzed to obtain (S)-5-{(4-[{(allyloxy)carbonyl}amino]butyl) (2,4-dimethoxybenzyl)amino}-2-{(*tert*-butoxycarbonyl)amino}-5-oxopentanoic acid (Compound 5). Furthermore, by substituting the Boc group of Compound 5 with an Fmoc group, the glutamine derivative of Formula (V) can be obtained. Commercially available reagents can be used for all of the reagents necessary to carry out Scheme (IV).

[0038]

On the other hand, synthesis of a stapled ERAP by Scheme (II) can be carried out using the glutamic acid derivative of Formula (IV) and the glutamine derivative of Formula (V) above, for example, as described below. First, a peptide is synthesized by standard Fmoc solid-phase peptide synthesis, with each one of the amino acid residues of a pair, at a position where one wants to form a stapling structure in the amino acid sequence of SEQ ID NO: 4 or SEQ ID NO: 5, being substituted with the glutamic acid derivative of Formula (IV) and the glutamine derivative of Formula (V), respectively. Then, the Fmoc-protected peptide is mixed with a solution of tetrakis(triphenylphosphine)palladium ($Pd(PPh_3)_4$) in $CHCl_3$/AcOH/*N*-methylmorpholine to reduce the substituent of the glutamine derivative residue. Next,

intramolecular amidation is carried out by using *N*,*N*-diisopropylcarbodiimide (DIPCDI) and 1-hydroxy-1H-benzotriazole hydrate (HOBt·H_2O) to couple the glutamine derivative residues. Furthermore, deprotection of acid-labile protecting groups and cleavage of peptides from resin are performed using a cocktail of TFA/*m*-cresol/thioanisole/1,2-ethanedithiol/H_2O. Following these, stapled ERAPs or sh stapled ERAPs carrying the stapling structure of Formula (I) (the double line drawn by a solid line and a dashed line is a single bond) can be obtained. In the stapled ERAP or sh stapled ERAP synthesized by Scheme (II), the number of amino acid residues interpositioned within the stapling structure is not particularly limited, but normally the preferred number is three residues.

[0039]

After introducing the first stapling structure (i.e., the first pair), similar reactions can be repeated to synthesize the peptide chain up to the position where the next stapled structure (i.e., the second pair) is to be introduced. Subsequently, by a second intramolecular crosslinking reaction, the stapling structure for the second pair is yielded. To further increase the number of crosslinking structures, structures of interest can be obtained by repeating similar reactions. Alternatively, two (or more) of peptide fragments to each of which a single stapling structure is introduced may be linked to produce a peptide introduced with two (or more) stapling structures.

Therefore, in a certain embodiment, the two pairs of amino acid residues substituted by stapling structures are at least adjacent to each other, or are independently positioned with one or more amino acid residues interposed inbetween them. More specifically, amino acid residues present within a single stapling structure are normally not substituted by another stapling structure. For example, when introducing stapling structures for two pairs, the number of amino acid residues present between the stapling structures may be, for example, zero (i.e., adjacent), one, two, or three. Considering the conditions such as the above, a peptide having a favorable structure in the present invention includes a peptide in which a pair of amino acid residues at a N-terminal side and, zero to three residues apart from it, a second pair of amino acid residues positioned at a C terminal side in the amino acid sequence of SEQ ID NO: 4 or 5 are each substituted with a stapling structure. Furthermore, by designing such that at least one amino acid residue constituting the amino acid pairs is L, the peptide is expected to become resistant to the actions of chymotrypsin.

[0040]

Specific structural examples of the peptides of the present invention include structures comprising at least two stapling structures, which are represented by Formula (II) shown below:

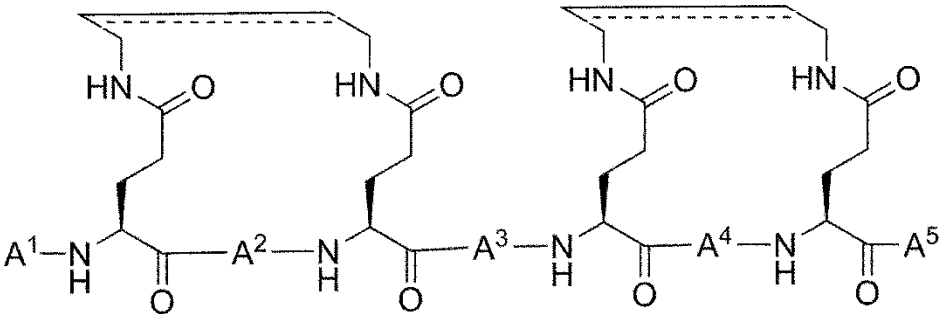

(II)

(wherein, the double line drawn by a solid line and a dashed line indicates a single bond or a double bond;

the combination of A^1, A^2, A^3, A^4, and A^5 is selected from the following:

A^1 = QM, A^2 = SDL, A^3 = –, A^4 = QLR, and A^5 = R; and

A^1 = QM, A^2 = SDL, A^3 = LQ, A^4 = RQR, and A^5 = OH;

wherein "–" indicates a peptide bond with no additional amino acid residue (that is, two stapling structures are connected); and

"OH" indicates that one end of the above stapling structure constitutes the C terminus of the peptide derivative).

[0041]

The peptides comprising two stapling structures, which are represented by Formula (II) above, may also be referred to as peptides formed by substituting each of the two pairs of amino acid residues (a) and (b) below by the stapling structure of Formula (I) in the peptide consisting of the amino acid sequence of SEQ ID NO: 4 (QMLSDLTLQLRQR):

(a) the third (L) and seventh (T) amino acid residues from the N terminus of the amino acid sequence of SEQ ID NO: 4; and

(b) the eighth (L) and twelfth (Q) amino acid residues from the N terminus of the amino acid sequence of SEQ ID NO: 4.

[0042]

Alternatively, they are peptides formed by substituting the two pairs of amino acid residues (c) and (d) below by the stapling structure of Formula (I) in the peptide consisting of the amino acid sequence of SEQ ID NO: 5 (QMLSDLTLQLRQRQ):

(c) the third (L) and seventh (T) amino acid residues from the N terminus of the amino acid sequence of SEQ ID NO: 5; and

(d) the tenth (L) and fourteenth (Q) amino acid residues from the N terminus of the amino acid sequence of SEQ ID NO: 5.

[0043]

Among the peptides comprising at least two stapling structures, which are represented by Formula (II), particularly preferred peptides include peptides in which the combination of A^1,

A^2, A^3, A^4, and A^5 in Formula (II) is selected from the following:

A^1 = QM, A^2 = SDL, A^3 = –, A^4 = QLR, and A^5 = R; and

A^1 = QM, A^2 = SDL, A^3 = LQ, A^4 = RQR, and A^5 = OH;

wherein "–" indicates a peptide bond with no additional amino acid residue (that is, two stapling structures are connected); and

"OH" indicates that one end of the above stapling structure constitutes the C terminus of the peptide derivative);

These peptides correspond to the following peptides:

(i) peptides formed by substituting each of the two pairs of amino acid residues (a) and (b) below by the stapling structure of Formula (I) in the peptide consisting of the amino acid sequence of SEQ ID NO: 4 (QMLSDLTLQLRQR):

(a) the third (L) and seventh (T) amino acid residues from the N terminus of the amino acid sequence of SEQ ID NO: 4; and

(b) the eighth (L) and twelfth (Q) amino acid residues from the N terminus of the amino acid sequence of SEQ ID NO: 4; or

(ii) peptides formed by substituting each of the two pairs of amino acid residues (c) and (d) below by the stapling structure of Formula (I) in the peptide consisting of the amino acid sequence of SEQ ID NO: 5 (QMLSDLTLQLRQRQ):

(c) the third (L) and seventh (T) amino acid residues from the N terminus of the amino acid sequence of SEQ ID NO: 5; and

(d) the tenth (L) and fourteenth (Q) amino acid residues from the N terminus of the amino acid sequence of SEQ ID NO: 5.

[0044]

Peptides of the present invention encompass peptides in which either or both of the N-terminal and C-terminal amino acid residues have been modified. The types of modifications are not particularly limited, but those that do not affect the affinity for PHB2 or cell permeability are preferred. Examples of preferred modifications include acetylation of the N-terminal amino acid residue, amidation of the C-terminal amino acid residue, addition of tag peptides such as HA-tag and FLAG-tag, and such. Furthermore, particularly preferred examples of the peptides of the present invention include peptides in which the N-terminal amino acid residue is acetylated and the C-terminal amino acid residue is amidated in the peptide represented by Formula (II) above. Amino acid residues other than the N-terminal and C-terminal amino acid residues are preferably not modified.

[0045]

The peptides of the present invention are not limited to those composed of L-amino acids and may be peptides including one or more D-amino acids. The composition ratio of L-

amino acids and D-amino acids in a peptide is not particularly limited, but for maintaining an α-helical structure, it is preferred that all amino acid residues are of the L-form (hereinafter, "L-form peptide") or all amino acid residues are of the D-form (hereinafter, "D-form peptide"). Therefore, in any one of the above-mentioned peptides of the present invention, peptides in which all amino acid residues have been substituted with D-form amino acid residues are also included as preferred embodiments of the peptides of the present invention. When the peptides of the present invention are D-form peptides, examples of preferred peptides may include peptides in which all amino acid residues in the peptides represented by Formula (II) have been substituted with D-form amino acid residues.

[0046]

Furthermore, the peptides of the present invention may be retro-inverso forms of any of the above-mentioned peptides of the present invention. A retro-inverso form has an amino acid sequence that is reversed from that of the original peptide, and all amino acid residues are substituted with D-form amino acid residues. More specifically, a retro-inverso form is a D-form peptide having an amino acid sequence that is reversed from that of the original peptide. Therefore, peptides which are retro-inverso forms of any one of the above-mentioned peptides of the present invention are included as preferred embodiments of the peptides of the present invention. When the peptides of the present invention are retro-inverso forms, examples of preferred peptides include peptides which are the retro-inverso forms of the peptides represented by Formula (II).

[0047]

When the peptides of the present invention are D-form peptides, D-form stapled ERAPs or sh stapled ERAPs can be synthesized by using D-amino acids instead of L-amino acids in methods as described above. In the synthesis of D-form stapled ERAPs or sh stapled ERAPs, D-form amino acid derivatives are used as the amino acid derivatives for forming stapling structures. Some of the D-form amino acid derivatives that can be used for forming stapling structures are commercially available. Therefore, such commercially available D-form amino acid derivatives may be used.

[0048]

Furthermore, when synthesizing D-form stapled ERAP by Scheme (I) shown in Fig. 7, a D-form optical isomer of the glutamine derivative represented by Formula (III) (hereinafter, "D-glutamine derivative of Formula (III)") may be used as the amino acid derivative for stapling. The D-glutamine derivative of Formula (III) can be synthesized by using *N*-α-(*tert*-butoxycarbonyl)-D-glutamic acid α methyl ester instead of *N*-α-(*tert*-butoxycarbonyl)-L-glutamic acid α methyl ester (Compound 3) in the above-mentioned Scheme (III). Then, a D-form stapled ERAP can be obtained by synthesizing a D-form peptide through standard Fmoc

solid-phase peptide synthesis using D-amino acids, with each amino acid residue of a pair at a position where one wants to form a stapling structure in the amino acid sequence of SEQ ID NO: 4 or SEQ ID NO: 5 being substituted with the D-glutamine derivative of Formula (III), and performing an olefin metathesis reaction according to Scheme (I). When synthesizing the retro-inverso form of a stapled ERAP or a sh stapled ERAP, solid-phase peptide synthesis can be performed based on the reversed amino acid sequence of the amino acid sequence of SEQ ID NO: 4 or 5 or a partial sequence thereof. Likewise the above, in this case too each amino acid residue of a pair, at a position where one wants to form a stapling structure, is substituted with the D-glutamine derivative of Formula (III) and then an olefin metathesis reaction is performed after synthesizing the peptide.

[0049]

When synthesizing a D-form stapled ERAP by Scheme (II) shown in Fig. 8, the D-form optical isomer of the glutamic acid derivative represented by Formula (IV) (hereinafter, "D-glutamic acid derivative of Formula (IV)") and the D-form optical isomer of the glutamine derivative represented by Formula (V) (hereinafter, "D-glutamine derivative of Formula (V)") can be used as the amino acid derivatives for stapling. Commercially available products can be used for the D-glutamic acid derivative of Formula (IV). The D-glutamine derivative of Formula (V) can be synthesized by using *N*-α-(*tert*-butoxycarbonyl)-D-glutamic acid α methyl ester instead of *N*-α-(*tert*-butoxycarbonyl)-L-glutamic acid α methyl ester (Compound 3) in Scheme (IV) shown in Fig. 6. Then, a D-form stapled ERAP can be obtained by synthesizing a D-form peptide through standard Fmoc solid-phase peptide synthesis using D-amino acids, with each one of the amino acid residues of a pair at a position where one wants to form a stapling structure in the amino acid sequence of SEQ ID NO: 4 or SEQ ID NO: 5 being substituted with the D-glutamic acid derivative of Formula (IV) and the D-glutamine derivative of Formula (V) respectively, and performing an intramolecular amidation reaction according to Scheme (II). When synthesizing the retro-inverso forms of stapled ERAPs, solid-phase peptide synthesis can be performed based on the reversed amino acid sequence of the amino acid sequence of SEQ ID NO: 4 or SEQ ID NO: 5. Likewise the above, in this case too each amino acid residue of a pair at a position where one wants to form a stapling structure is substituted with the D-glutamic acid derivative of Formula (IV) and the D-glutamine derivative of Formula (V), respectively, and then an intramolecular amidation reaction is performed after synthesizing the peptide.

[0050]

Peptides of the present invention may also be in the form of salts. The form of salts is not particularly limited, but pharmaceutically acceptable salts are preferred. Herein, the "pharmaceutically acceptable salt" refers to a salt that retains the pharmacological and

pharmaceutical efficacy and characteristics of a peptide. Preferred examples of salts include salts with alkali metals (lithium, potassium, sodium and such), salts with alkaline-earth metals (calcium, magnesium and such), salts with other metals (copper, iron, zinc, manganese and such), salts with organic bases, salts with amines, salts with organic acids (acetic acid, formic acid, propionic acid, fumaric acid, maleic acid, succinic acid, tartaric acid, citric acid, malic acid, oxalic acid, benzoic acid, methanesulfonic acid, and such), salts with inorganic acids (hydrochloric acid, phosphoric acid, hydrobromic acid, sulfuric acid, nitric acid and such), and such. These salts can be prepared according to known methods.

[0051]

Pharmaceutical compositions

Peptides or salts thereof of the present invention can be formulated as pharmaceutical compositions along with pharmaceutically acceptable carriers.

[0052]

Peptides of the present invention have a binding ability to PHB2, and competitively inhibit the BIG3-PHB2 interaction. The formation of BIG3-PHB2 complex enhances estrogen-dependent transcriptional activity and induces proliferation of cancer cells. Therefore, peptides of the present invention which suppress the formation of BIG3-PHB2 complex by inhibiting the BIG3-PHB2 interaction are useful as pharmaceutical compositions for cancer therapy in particular.

[0053]

Enhancement of estrogen-dependent transcriptional activity by the formation of BIG3-PHB2 complex takes place mainly in estrogen receptor-positive cells. Therefore, peptides of the present invention are useful as pharmaceutical compositions for therapy of estrogen receptor-positive cancer in particular. Examples of such estrogen receptor-positive cancer include breast cancer, endometrial cancer, ovarian cancer, prostate cancer (Nelles JL, *et al.*, Expert Rev Endocrinol Metab. 2011 May; 6(3): 437-451), and lung cancer (particularly non-small-cell lung cancer) (Stabile LP, *et al.*, Cancer Res. 2005 Feb 15; 65(4): 1459-70; Marquez-Garban DC, *et al.*, Steroids. 2007 Feb; 72(2): 135-43), but are not limited thereto. Cancers to which pharmaceutical compositions of the present invention are applied preferably express BIG3 and PHB2, and estrogen receptor-positive cancers generally express BIG3 and PHB2. Whether a cancer is estrogen receptor-positive can be confirmed by known methods such as ELISA or immunohistochemical staining.

[0054]

Furthermore, peptides of the present invention have growth suppressive effects on tamoxifen-resistant estrogen receptor-positive cancers as well. Therefore, pharmaceutical compositions of the present invention may also be applied to tamoxifen-resistant estrogen

receptor-positive cancers. An example of tamoxifen-resistant estrogen receptor-positive cancers to which pharmaceutical compositions of the present invention will be applied includes tamoxifen-resistant estrogen receptor-positive breast cancer. Therefore, an example of preferred subjects to whom a pharmaceutical composition of the present invention is to be administered includes patients with tamoxifen-refractory estrogen receptor-positive breast cancer.

Furthermore, the peptides of the present invention showed inhibitory effects on the growth of breast cancer cells having a mutation in the estrogen receptor (ESR1). The mutation in ESR1 is considered as one mechanism for the acquisition of resistance to hormone therapy. Furthermore, the peptides of the present invention showed excellent cell growth inhibitory effects in triple-negative breast cancer cells (Fig. 30). Generally, triple-negative refers to breast cancer cells lacking expression of HER2, estrogen receptors, and progesterone receptors, which are targeted factors in major drug therapies. Therefore, triple-negative breast cancers are normally resistant to drug therapy. In addition, the present inventors discovered that the peptides of the present invention have high cell growth inhibitory effects against cells of HER2-positive breast cancer which is generally known as highly malignant breast cancer. Therefore, the peptides of the present invention are useful as pharmaceutical compositions for administration to patients with such treatment-resistant or malignant breast cancers.

More specifically, the present invention provides pharmaceutical compositions comprising a peptide of the present invention, which are for administration to either or both of drug therapy-resistant breast cancer patients and malignant breast cancer. The present invention also relates to peptides of the present invention for use in treatment of either or both of drug therapy-resistant breast cancer patients and malignant breast cancer. Furthermore, the present invention relates to use of the peptides of the present invention in the production of pharmaceutical compositions for treating either or both of drug therapy-resistant breast cancer patients and malignant breast cancer. The present invention also provides methods for treating breast cancer which comprise the steps of selecting patients having either or both of drug therapy-resistant breast cancer and malignant breast cancer, and administering a peptide of the present invention to the selected patients.

Patients with drug therapy-resistant breast cancer can be identified by observing the therapeutic outcome after common drug therapy. Specifically, when degeneration of the disease focus is not clearly observed by the treatment, one can know that this cancer is treatment-resistant. A condition where enlargement of the disease focus is prevented is included in the degeneration of the disease focus. Alternatively, markers for predicting the malignancy of breast cancer are known. When such markers are detected, one can know that the patient has highly malignant breast cancer. For example, HER2 is one indicator for malignant breast

cancer. Furthermore, triple-negative breast cancer patients are said to have resistance to drug therapies. Triple-negative refers to breast cancers having the features of lacking expression of estrogen receptors and progesterone receptors in addition to the aforementioned HER2. These markers for malignancy and drug therapy resistance can be evaluated quantitatively by immunostaining and gene expression profiling. For example, the marker status is determined to be negative when the expression level is approximately the same as that of a negative control. For the negative control, treatment-resistant cancer cell lines lacking expression of these markers can be used.

[0055]

Pharmaceutical compositions of the present invention can be produced using known drug formulation techniques by mixing a peptide or a salt thereof of the present invention with a pharmaceutically acceptable carrier. Herein, "pharmaceutically acceptable carrier" refers to an inactive substance to be used as diluents or solvents for drugs. For the pharmaceutically acceptable carriers to be used in pharmaceutical compositions of the present invention, carriers generally used for pharmaceutical products can be appropriately selected according to the dosage form of the pharmaceutical compositions to be prepared.

[0056]

The dosage forms of the pharmaceutical compositions of the present invention are not particularly limited, and dosage forms generally used for pharmaceutical products such as liquids, tablets, elixirs, capsules, granules, and powders can be selected appropriately. Furthermore, depending on the selected dosage form, additives such as excipients, stabilizers, suspensions, preservatives, surfactants, solubilizing agents, pH adjusters, and aggregation inhibitors can be added appropriately.

[0057]

Pharmaceutical compositions of the present invention contain a pharmaceutically effective amount of peptides or salts thereof of the present invention. The pharmaceutically effective amount can be selected appropriately according to the dosage form of the pharmaceutical compositions, dosage interval, age, gender, body weight, and body surface area of subjects for administration, type of disease, and such. Examples of the content of peptides or salts thereof of the present invention in pharmaceutical compositions of the present invention include 0.001 mg to 1000 mg, 0.01 mg to 100 mg, 0.1 mg to 30 mg, or 0.1 mg to 10 mg, but are not limited thereto.

[0058]

Pharmaceutical compositions of the present invention may optionally include other pharmaceutical agents. Examples of other pharmaceutical agents include anti-inflammatory agents, analgesic agents, antipyretics, other therapeutic agents for cancer, and such. Other

therapeutic agents for cancer that may be used for pharmaceutical compositions of the present invention are not particularly limited, but when the pharmaceutical compositions are used for estrogen-positive cancers, examples may include hormone therapy agents such as selective ERα modulators (*e.g.*, tamoxifen and raloxifene), ERα down-regulators (*e.g.*, fulvestrant), aromatase inhibitors, LH-RH agonist formulations, and progesterone formulations. These pharmaceutical agents may also be mixed in the form of prodrugs and pharmaceutically acceptable salts.

[0059]

Pharmaceutical compositions of the present invention can be administered to a subject by appropriately selecting a suitable administration route depending on the dosage form. The administration route is not particularly limited, but examples include oral administration, intradermal, subcutaneous, intramuscular, intraosseous, peritoneal and intravenous injection, and such. Furthermore, while either systemic administration or local administration near the diseased site is possible, local administration is preferred. More specifically, pharmaceutical compositions of the present invention can be administered by means of injection and such to the cancer tissue or to its vicinity. Alternatively, pharmaceutical compositions of the present invention can be administered surgically into the cancer tissue or to its vicinity. Pharmaceutical compositions of the present invention can also be prepared as a controlled-release preparation by combining them with appropriate carriers.

[0060]

Dosage interval of pharmaceutical compositions of the present invention may also be appropriately selected according to the age, gender, body weight, and body surface area of subjects for administration, the disease type and such, as well as the dosage form, administration route, and such of the pharmaceutical compositions of the present invention. Examples of the dosage interval include every day, every four days, and every seven days, but are not limited thereto.

[0061]

Dosage of pharmaceutical compositions of the present invention may also be appropriately selected according to the age, gender, body weight, and body surface area of subjects for administration, the disease type and such, as well as the dosage form, administration route, and such of the pharmaceutical compositions of the present invention.

Examples of the dosage of peptides or salts thereof of the present invention include, for example, 0.001 mg/kg/day to 1000 mg/kg/day, 0.005 mg/kg/day to 500 mg/kg/day, 0.01 mg/kg/day to 250 mg/kg/day, but are not limited thereto.

[0062]

Pharmaceutical compositions of the present invention may be used in combination with other pharmaceuticals depending on the condition of the administration subjects. The

pharmaceuticals used in combination are not particularly limited, but when the pharmaceutical compositions are used for estrogen receptor-positive cancers, examples may include hormone therapy agents such as selective ERα modulators (*e.g.*, tamoxifen and raloxifene), ERα down-regulators (*e.g.*, fulvestrant), aromatase inhibitors, LH-RH agonist formulations, and progesterone formulations. Among these hormone therapy agents, particularly preferred examples include tamoxifen and fulvestrant.

[0063]

When pharmaceutical compositions of the present invention are used for cancer therapy, one may examine whether the cancer to be treated is accompanied by expression of BIG3 and PHB2 before administering the pharmaceutical compositions. Whether BIG3 and PHB2 are expressed in the cancer to be treated can be confirmed by detecting transcription products or translation products of these genes in the samples collected from the subjects. Known methods can be used for detection methods, and for example, methods of detecting transcription products using probes or PCR methods (for example, cDNA microarray method, Northern blotting, and RT-PCR) and methods of detecting translation products using antibodies and such (for example, Western blotting and immunostaining) may be used.

[0064]

The present invention also provides articles of manufacture or kits that comprise a pharmaceutical composition of the present invention. The articles of manufacture or kits of the present invention can include a container that houses the pharmaceutical composition of the present invention. An example of an appropriate container includes a bottle, a vial or a test tube, but is not limited thereto. The container may be formed of various materials such as glass or plastic. A label may be attached to the container, and the disease or disease state to which the pharmaceutical composition of the present invention should be used may be described in the label. The label may also indicate directions for administration and such.

[0065]

The articles of manufacture or kits of the present invention may further comprise a second container that houses pharmaceutically acceptable diluents optionally, in addition to the container that houses the pharmaceutical composition of the present invention. The articles of manufacture or kits of the present invention may further comprise the other materials desirable from a commercial standpoint and the user's perspective, such as the other buffers, diluents, filters, injection needles, syringes, and package inserts with instructions for use.

[0066]

As needed, the pharmaceutical composition of the present invention can be provided in a pack or dispenser device that can contain one or more units of dosage forms containing active ingredients. The pack can include, for example, a metallic foil or a plastic foil such as a blister

pack. Instructions for administration can be attached to the pack or dispenser device.

[0067]

In another embodiment, the present invention provides the following use, methods, and such:

(a) use of a peptide or a salt thereof of the present invention in the production of a pharmaceutical composition for cancer therapy;

(b) a peptide or a salt thereof of the present invention for use in cancer therapy;

(c) a method or process for producing a pharmaceutical composition for cancer therapy, which comprises the step of formulating a peptide or a salt thereof of the present invention with a pharmaceutically acceptable carrier;

(d) a method or process for producing a pharmaceutical composition for cancer therapy, which comprises the step of mixing a peptide or a salt thereof of the present invention with a pharmaceutically acceptable carrier; and

(e) a method for cancer therapy, which comprises administering a peptide or a salt thereof of the present invention to a subject.

[0068]

Hereinbelow, the present invention is described in more detail with reference to the Examples. Nevertheless, while the following materials, method and Examples may serve to assist one of ordinary skill in making and using certain embodiments of the present invention, there are only intended to illustrate aspects of the present invention and thus in no way to limit the scope of the present invention. One of ordinary skill in the art can use methods and materials similar or equivalent to those described herein in the practice or testing of the present invention.

[0069]

All prior art documents cited herein are incorporated by reference in the present specification.

[Example]

[0070]

[Example 1] Synthesis of Double Stapled Peptides

Synthesis of double stapled ERAP No. 45 (SEQ ID NO: 2) and stapled ERAP No. 46 (SEQ ID NO: 3)

Peptide chain elongation was performed using the Rink Amide AM Resin (content: 0.62 mmol amine/g) by Fmoc solid-phase peptide synthesis method. Unnatural amino acids Xs (X^1 = Fmoc-Glu(OAllyl)-OH; X^2 = Fmoc-Glu(N(DMB)-$CH_2CH_2CH_2CH_2$-NH-Alloc)-OH) were introduced at sites necessary for stapling $QMX^1SDLX^2X^1QLRX^2R$ which is the precursor

sequence of double stapled ERAP No. 45 and $QMX^1SDLX^2LQX^1RQRX^2$ which is the precursor sequence of double stapled ERAP No. 46. For natural amino acids, Fmoc-Gln(Trt)-OH, Fmoc-Met-OH, Fmoc-Ser(*t*Bu)-OH, Fmoc-Asp(O*t*Bu)-OH, Fmoc-Leu-OH, and Fmoc-Arg(Pbf)-OH were respectively used at three equivalents relative to the resin. *O*-benzotriazolyl-*N'*,*N'*,*N'*,*N'*-tetramethyluronium hexafluorophosphate (HBTU; 0.99 equivalents relative to the amino acid) and *N*,*N*-diisopropylethylamine (DIPEA; 2 equivalents relative to the amino acid) in *N*,*N*-dimethylformamide (DMF) was used for activation at room temperature for 30 seconds, and this was made to react with the amino groups on the solid resin at room temperature for 2 hours. For unnatural amino acids Xs, the amino acid was used at 1.5 equivalents relative to the resin, and by similarly using HBTU as the activator, this was reacted at room temperature for 2 hours. Cleavage of the Fmoc group was carried out by treatment with a solution of 20% piperidine in DMF at room temperature for ten minutes.

[0071]

Stapling was performed when a set of X^1 and X^2 was introduced from the C-terminal side. More specifically, under an Ar atmosphere, allyl and alloc groups were removed from N^{α}-Fmoc-protected peptide resins by adding $Pd(PPh_3)_4$ (3 equivalents) and stirring at room temperature for 12 hours (performed twice) in a mixed solvent of *N*-methylmorpholine (10 equivalents)/AcOH/$CHCl_3$ (0.5:2:37.5 (v/v)). After removing the protecting groups, the resins were washed using $CHCl_3$, DMF, 1 M sodium dimethyldithiocarbamate/DMF (semicarbazide solution), $CHCl_3$, DMF, and 1 M 1-hydroxybenzotriazole (HOBt)·H_2O/NMP (only after the second deprotection) in that order. Then, in *N*-methyl-2-pyrrolidone (NMP), 1 M HOBt·H_2O/NMP (10 equivalents) and DIPCI (10 equivalents) were added and this mixture was reacted at room temperature for 24 hours for intramolecular amide bond formation. For the second stapling, a similar method as described above was performed on the N^{α}-acetylated resin after completion of resin elongation. Furthermore, the N terminus was acetylated using $(AcO)_2O$ (10 equivalents relative to the amino acid) and DIPEA (10 equivalents relative to the amino acid).

[0072]

The resins that have completed amino acid elongation and side chain stapling were treated with TFA/thioanisole/*m*-cresol/1,2-ethanediol (EDT)/H_2O (80:5:5:5:5 (v/v), 50 μL of deprotection reaction solution for 1 mg of resin) at room temperature for 2 hours to cleave the side-chain protecting groups. The reaction solution was concentrated, then Et_2O was added, and the crude peptide was precipitated. This was washed with Et_2O three times to yield samples for HPLC purification. The conditions for peptide purification and the results from mass spectrometry are as shown below.

[0073]

Double stapled ERAP No. 45
Column: Cosmosil 5C_{18} (10 x 250 mm); Solvent:
A 0.1% TFA-H_2O, B 0.1% TFA in CH_3CN,
B (10%-45% over 30 min) in solvent A;
Flow: 3.0 mL/min; Detect: 220 nm,
Retention time 24.5 min
MS m/z calcd for $C_{76}H_{130}N_{26}O_{23}S$ $[M+2H]^+$ 904.5,
found 904.6

Double stapled ERAP No. 46
Column: Cosmosil 5C_{18} (10 x 250 mm); Solvent:
A 0.1% TFA-H_2O,
B 0.1% TFA in CH_3CN, B (10%-45% over 30 min) in solvent A;
Flow: 3.0 mL/min; Detect: 220 nm,
Retention time 19.8 min
MS m/z calcd for $C_{81}H_{138}N_{28}O_{25}S$ $[M+2H]^+$ 968.5,
Found 968.6

[0074]

Structures of unnatural amino acids X^1 and X^2 (X^1=Fmoc-Glu(OAllyl)-OH; X^2=Fmoc-Glu(N(DMB)-$CH_2CH_2CH_2CH_2$-NH-Alloc)-OH)

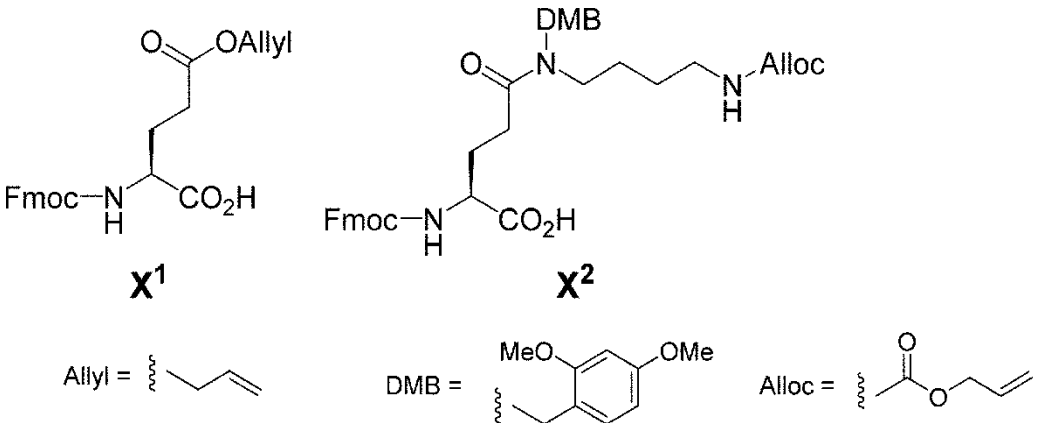

[0075]

[Example 2] Effects of Double Stapled ERAPs on Estrogen-dependent Breast Cancer Cells

Materials and Methods

Cell lines and Culturing Conditions

Human breast cancer cell line MCF-7 was purchased from JCRB Cell Bank (Osaka, Japan) and mammary epithelial cell line MCF-10A was purchased from American Type Culture Collection (ATCC, Manassas, VA, USA). Both cell lines were maintained in an appropriate

medium under 5% CO_2 at 37°C.

For cell growth assays, the respective cells were seeded into 48-well plates (2 x 10^4 cells/200 μL), and for immunoprecipitation, the respective cells were seeded into 10-cm dishes (2 x 10^6 cells/10 mL).

MCF-7 cells were seeded in MEM (Thermo Fisher Scientific) supplemented with 10% FBS (Nichirei Biosciences Inc., Tokyo, Japan), 1% Antibiotic/Antimycotic solution (Thermo Fisher Scientific, Waltham, MA, USA), 0.1 mM NEAA (Thermo Fisher Scientific), 1 mM sodium pyruvate (Thermo Fisher Scientific), and 10 μg/mL insulin (Sigma, St. Louis, MO, USA). MCF-10A cells were seeded in MEBM (Lonza) supplemented with a Single Quots kit (BPE, hydrocortisone, hEGF, insulin, gentamycin/amphoterin-B) (Lonza, Walkersville, MD, USA) and 100 ng/mL cholera toxin. For 17β-estradiol (estrogen, Sigma) stimulation, the medium for MCF-7 cells was changed to phenol red-free DMEM/F12 (Thermo Fisher Scientific) supplemented with 10% FBS, 1% Antibiotic/Antimycotic solution, 0.1 mM NEAA, 1 mM sodium pyruvate, and 10 μg/mL insulin on the next day after seeding. 24 hours later, the cells were treated with 10 nM estrogen alone or with 10 nM estrogen and a peptide (a single stapled ERAP or a double stapled ERAP).

[0076]

Cell Growth Assay

Cell growth assays on MCF-7 and MCF-10A were carried out using the Cell Counting Kit-8 (CCK-8) (Dojindo, Kumamoto, Japan). The data are shown by mean ± standard deviation of three independent experiments.

[0077]

Chymotrypsin Resistance

Chymotrypsin resistance was analyzed by adding 1 μg of chymotrypsin (#C7761, Sigma) and 5 μg of double stapled ERAP in a buffer (50 mM Tris-HCl; pH 8.0, 10 mM $CaCl_2$), allowing this to react at 37°C for 24 hours, and then subjecting the whole amount to high-performance liquid chromatography (HPLC). For the HPLC, a reverse-phase column (Inertsil Peptides C18 250 x 3.0 mm I.D.; GL Science, Tokyo, Japan) was used, gradient elution was performed using Solution A (0.1% trifluoroacetic acid) and Solution B (0.1% trifluoroacetic acid/acetonitrile) (A/B = 90/10 (0 - 20min), 90/10 - 40/60 (20 - 80min)) at a flow rate of 0.3 mL/min, and a chromatogram for each double stapled ERAP was obtained by UV detection at 210 nm.

[0078]

Antibodies and Immunoblot Analyses

For immunoblot analyses, after performing SDS-PAGE, the membranes blotted with proteins were blocked with 4% BlockAce solution (Dainippon Pharmaceutical, Osaka, Japan) for

3 hours and then incubated to react for 12 hours with antibodies against BIG3 (1:1,000) and PHB2 (1:1,000) (Abcam, Cambridge, UK). After allowing interaction with HRP-labeled secondary antibodies (anti-rat IgG-HRP for BIG3, 1:5,000; and anti-rabbit IgG-HRP for PHB2, 1:1,000) (Santa Cruz Biotechnology, Dallas, TX, USA) for 1 hour, the blots were developed with the Enhanced Chemiluminescence (ECL) system (GE Healthcare, Buckinghamshire, UK) and scanned using the Image Reader LAS-3000 mini (Fujifilm, Tokyo, Japan).

[0079]

Immunoprecipitation

For immunoprecipitation analysis, cell lysates lysed in a cell lysis buffer (50 mM Tris-HCl; pH 8.0, 150 mM NaCl, 0.1% NP-40, and 0.5% CHAPS; 0.1% protease inhibitor cocktail III) were pre-cleared with a rat IgG antibody and rec-Protein G Sepharose 4B (Thermo Fisher Scientific) at 4°C for 3 hours. Then, the supernatants were incubated for reaction with 5 μg of an antibody against BIG3 at 4°C for12 hours. Next, the antigen-antibody complexes were precipitated using rec-Protein G Sepharose 4B at 4°C for 1 hour. The immunoprecipitated protein complexes were washed four times with the cell lysis buffer. Then, SDS-PAGE and immunoblot analyses were carried out.

[0080]

Results

Synthesis of Double Stapled ERAP (see the method for synthesizing double stapled ERAPs of Example 1)

Stable long-term inhibition of estrogen-dependent tumor growth was possible with single stapled ERAP (SEQ ID NO: 1); however, further enhancement of stability was undertaken by increasing the number of intramolecular crosslinks. The positions for the intramolecular crosslinks were designed to crosslink leucine residues by considering resistance to chymotrypsin, and double stapled ERAPs having, in addition to the crosslinking position for single stapled ERAP (167L and 171T), a crosslink between 172L and 175Q (Fig. 1, double stapled ERAP No. 45) and a crosslink between 174L and 178Q (Fig. 1, double stapled ERAP No. 46) were synthesized.

[0081]

Long-term Stability of Double Stapled ERAPs on Estrogen-dependent Growth

96-hour treatment with single stapled ERAP suppressed the growth of estrogen-dependent MCF-7 cells in a concentration-dependent manner, and the IC_{50} was 0.88 μM. Treatment with double stapled ERAP No. 45 at 10 μM for 96 hours sustained almost complete suppressive effects; however, up to 1 μM, estrogen-dependent cell growth could hardly be suppressed, its inhibitory effect was inferior to that of single stapled ERAP (IC_{50} = 2.32 μM, Fig. 2A). This indicates the possibility that the three-dimensional structure of the continuous

stapling has an influence on membrane permeability and such. On the other hand, double stapled ERAP No. 46 was different from double stapled ERAP No. 45 in that its inhibitory effect on estrogen-dependent growth was stronger than that of the single stapled ERAP, and showed 81% inhibition rate even at 1 μM (Fig. 2B, single stapled ERAP: 51% inhibition rate; double stapled ERAP No. 45: 21% inhibition rate), and its IC_{50} was 0.43 μM which is two-fold enhanced than the single stapled ERAP (Fig. 2C).

[0082]

Chymotrypsin-resistance of Double Stapled ERAPs

Resistance of double stapled ERAPs No. 45 and No. 46 to treatment with chymotrypsin for 24 hours was examined. Proteolysis by chymotrypsin treatment is indicated by a black arrow in Fig. 3. The results show that while chymotrypsin treatment of double stapled ERAP No. 45 led to observation of several degradation products (Fig. 3A), chymotrypsin treatment of double stapled ERAP No. 46 hardly showed its degradation (Fig. 3B). Resistance to proteolysis by chymotrypsin treatment suggests that ERAP is resistant to degradation *in vivo*, and this may be reflected in maintenance of long-term stable inhibitory effects on estrogen-dependent cell growth.

[0083]

Effects of Double Stapled ERAP on Mammary Epithelial Cell Growth

Using 1 μM and 10 μM double stapled ERAP No. 46, effects on the growth of MCF-10A cells were examined. MCF-10A cell is an ERα-negative and BIG3-negative normal mammary epithelial cell. As a result, while treatment with 1 μM and 10 μM double stapled ERAP No. 46 for 96 hours showed inhibition rates of 79% and 91% on estrogen-dependent cell growth in ERα-positive and BIG3-positive MCF-7 breast cancer cells (Fig. 2B), there were hardly any effects on MCF-10A cell growth up to 10 μM (Fig. 4), and this suggested that the double stapling structure does not become involved in the functions of normal mammary epithelial cells.

[0084]

Binding Inhibition of the BIG3-PHB2 Interaction by Double Stapled ERAP No. 46

Inhibitory effect on the interaction between BIG3 and PHB2 was examined for treatment with 1 μM and 10 μM double stapled ERAP No. 46 for 24 hours and 96 hours. The results showed that 24-hour treatment with the double stapled ERAP at 1 μM nearly completely inhibited the binding between BIG3 and PHB2 (Fig. 5A); whereas, while 10 μM single stapled ERAP gave nearly complete inhibitory effect, 1 μM single stapled ERAP gave a decreased inhibition rate of 46% (Fig. 5A). Furthermore, treatment for 96 hours yielded inhibition rates of 60% and 95% for double stapled ERAP No. 46 at concentrations of 1 μM and 10 μM, respectively; therefore, while the values were slightly decreased compared to those from

treatment for 24 hours (Fig. 5B), strong inhibitory effects were sustained. On the other hand, inhibitory effects were hardly observed for single stapled ERAP at 1 μM, and the inhibition rate was 81% at 10 μM (Fig. 5B). From the above-mentioned facts, double stapled ERAP No. 46 can inhibit the binding between BIG3 and PHB2 at a concentration lower than that of single stapled ERAP, and as a result, it was determined to be able to suppress growth at a lower concentration.

[0085]

[Example 3] Effects of stERAP on ESR1 Mutant Breast Cancer Cells

Materials and Methods

Cell lines

MCF-7 cells and HEK293T cells were purchased from American Type Culture Collection (ATCC, Manassa, VA, USA). Y537S knock-in MCF-7 cells were provided by Dr. Laki Buluwela (Imperial College London, UK). All cell lines were cultured under conditions recommended by their respective depositors.

[0086]

Cell Culture

MCF-7 cells were cultured in MEM (Thermo Fisher Scientific) supplemented with 10% FBS (Nichirei Biosciences Inc., Tokyo, Japan), 1% Antibiotic/Antimycotic solution (Thermo Fisher Scientific, Waltham, MA, USA), 0.1 mM NEAA (Thermo Fisher Scientific), 1 mM sodium pyruvate (Thermo Fisher Scientific), and 10 μg/mL insulin (Sigma, St. Louis, MO, USA). HEK293T cells were cultured in DMEM (Sigma) supplemented with 10% FBS and 1% antibiotic/antimycotic solution. Y537S knock-in MCF-7 cells were cultured in DMEM (Sigma) supplemented with 10% FBS, 1% antibiotic/antimycotic solution, and 0.1 mM NEAA. The respective cells were seeded into 48-well plates (2×10^4 cells/0.2 mL), 6-well plates (5×10^5 cells/2 mL), or 10-cm dishes (2×10^6 cells/10 mL), incubated under 5% CO_2 at 37ºC, and treated with an inhibitor such as stERAP 24 hours later.

[0087]

Compounds and Inhibitors

For the peptide that inhibits the BIG3-PHB2 binding, the single stapled ERAP (stERAP, or stapled ERAP) described in WO 2017/12646 was used. Tamoxifen was purchased from Sigma, fulvestrant was purchased from LKT laboratories (St. Paul, MN, USA), and everolimus was purchased from Cell Signaling Technology (Danvers, MA, USA). Staurosporine and wortmannin were provided by OncoTherapy Science, Inc. (Kanagawa, Japan) and Dr. Takuya Sasaki (Tokushima University, Tokushima, Japan).

[0088]

Western Blot Analyses

Cells were lysed in a lysis buffer (50 mM Tris-HCl: pH 8.0, 150 mM NaCl, 0.1% NP-40, 0.5% CHAPS) containing 0.1% protease inhibitor cocktail III (Calbiochem, San Diego, CA, USA). The cell lysates were subjected to electrophoresis, transferred to nitrocellulose membranes by blotting. Then, the membranes were blocked with 4% BlockAce solution (Dainippon Pharmaceutical, Osaka, Japan) for 3 hours. The membranes were incubated for 12 hours in the presence of anti-FLAG tag antibody (M2) (Sigma); anti-PHB2 antibody (Abcam, Cambridge, UK); anti-PKCα antibody (H-7) and anti-PI3-kinase p85α (U13) (Santa Cruz Biotechnology, Santa Cruz, CA, USA); anti-phosphorylated PI3K p85/p55 antibody (Tyr458/Tyr199), anti-phosphorylated PKCα/βII antibody (Thr638/Thr641) (Cell Signaling Technology); anti-ERα antibody (SP1) (Thermo Fisher Scientific); or anti-phosphorylated PHB2 purified antibody (Ser39) (Scrum Inc., Tokyo, Japan). After incubation in the presence of HRP-conjugated secondary antibody (Santa Cruz Biotechnology) for 1 hour, the membranes were developed with an enhanced chemiluminescence system (GE Healthcare, Buckinghamshire, UK). The blots were scanned using the Image Reader LAS-3000 mini (Fujifilm, Tokyo, Japan).

[0089]

Immunoprecipitation

As described in the "Western Blot Analyses" section, the cells were lysed in a 0.1% NP-40 lysis buffer, and the cell lysates were pre-cleared with Normal IgG and rec-Protein G Sepharose 4B (Thermo Fisher Scientific) at 4°C for 3 hours. After centrifugation, the supernatants were incubated at 4°C for 12 hours in the presence of 5 μg of anti-PKCα antibody, anti-ERα antibody, or anti-FLAG-tagged antibody. After adding rec-Protein G Sepharose 4B and incubating at 4°C for 1 hour, the antigen-antibody complexes were precipitated. The immunoprecipitated protein complexes were washed three times with the lysis buffer and separated by SDS-PAGE. Thereafter, Western blot analyses were carried out.

[0090]

PKCα (Protein Kinase C alpha) Activity

PKCα activity was measured by reacting the immunoprecipitates by PKCα with a PHB2 peptide carrying the substrate Ser39 (YGVRESVFTVE (SEQ ID NO: 17)) and 0.5 mM ATP in a kinase buffer solution (25 mM Hepes, pH 7.2; 25 mM $MgCl_2$; 5 mM EDTA; 5 mM EGTA; 0.25 mM DTT) at 30°C for 30 minutes, and using the ADP-Glo kinase assay Kit (Promega, Fitchburg, WI, USA).

[0091]

Cell Growth Assay

Cell growth assay was carried out using the Cell Counting Kit-8 (CCK-8; Dojindo, Kumamoto, Japan). The cells were seeded into 48-well plates at 2 x 10^4 cells/well and maintained in an incubator (37°C) in the presence of 5% CO_2. At a point as instructed, a ten-

fold diluted CCK-8 solution was added, incubated for 30 minutes, and the absorbance at 450 nm was measured to calculate the number of viable cells.

[0092]

Luciferase Reporter Assay

To perform ERE reporter assay, an ERE reporter (SABiosciences, Frederick, MD, USA) was transfected into MCF-7 cells, and 16 hours after transfection, medium was exchanged to an assay medium (Opti-MEM, 10% FBS, 0.1 mM NEAA, 1 mM Sodium pyruvate, and 10 μg/mL insulin). 8 hours after the medium exchange, cells were treated with estrogen and stERAP for 24 hours. The cell lysates were evaluated for luciferase and Renilla-luciferase activities using the Promega dual luciferase reporter assay (Promega KK, Tokyo, Japan). Considering the transfection efficiency, all data were normalized to the Renilla-luciferase activity.

[0093]

Statistical Analyses

Student's t-tests were used to determine the statistical significance of the differences among the experimental groups. $P < 0.05$ was considered significant.

[0094]

Results

ESR1 Mutant Breast Cancer Cell Line Binds to PI3K Estrogen independently

An estrogen receptor (ERα) is expressed in 70% of breast cancers, and most of these cancers are sensitive to ERα inhibition. However, in ERα-positive advanced breast cancers, mutation of the ERα gene (ESR1) is manifested in the ligand-binding domain, such gene mutations are activated in a ligand independent manner, and such cancers are suggested to have the possibility of being resistant to endocrine therapy (Nat. Genet., 45, 1439, 2013; and Nat. Genet., 45, 1446, 2013). Furthermore, in ERα-positive breast cancers, the PI3K (phosphatidylinositol 3-kinase)/AKT (protein kinase B)/mTOR (mammalian target of rapamycin) pathway in addition to the estrogen signal has a very important function, and has been reported to be involved in the mechanism of resistance to endocrine therapy (Cancer Discov. 2011 Sep, 1(4): 338-51; Nature, e2012 Oct 4, 490(7418): 61-70; Cancer Lett. 2012 Oct 1, 323(1): 77-87; Clin. Breast Cancer. 2015 Jun, 15(3): 197-203). First, whether wildtype (WT) and mutant (Y537S) ESR1 bind to PI3K was examined. As a result, MCF-7 cells transfected with WT did not show any binding between ERα and PI3K in the absence of estrogen treatment; however, in the presence of estrogen, binding between ERα and PI3K, and phosphorylation of PI3K were observed (Fig. 9A). On the other hand, MCF-7 cells transfected with Y537S were different from cells transfected with WT, and even in the absence of estrogen treatment, PI3K bound to Y537S and was phosphorylated, and PKCα activation (phosphorylation of Thr638/Thr641) was observed (Fig. 9B). This suggests the possibility that structural changes

due to mutation of ESR1 enable estrogen-independent binding between the ESR1 mutant and PI3K, and cause acquisition of resistance. Furthermore, upon 10 μM stERAP treatment, PHB2 that had dissociated from BIG3 newly bound to Y537S even in the absence of estrogen, and while the amount of the bound PHB2 reached a maximum 1 hour after stERAP treatment, thereafter, phosphorylation of PI3K and PKCα decreased (Fig. 9B). Interestingly, phosphorylation of Ser39 of PHB2 was induced immediately after stERAP treatment and maximum phosphorylation intensity was indicated in 3 hours, the intensity thereafter weakened due to decrease in phosphorylated PI3K (negative regulation of the phosphorylated PHB2; Fig. 9B). However, in comparison to the phosphorylation intensities of PI3K and PKCα, phosphorylation of PHB2 (Ser39) maintained a certain level of intensity (Fig. 9B); thus, stERAP was considered to have suppressive effects on the ERα-Y537S resistant cells.

[0095]

ESR1 Mutant Breast Cancer Cell Line Has Estrogen-independent High PKCα Activity

Since ESR1 mutants bind to PI3K, it is suggested that the mutants activate PKC which is the downstream molecule of PI3K (Biochem. Biophys. Res. Commun., 310, 720, 2004). Furthermore, the present inventors have found that in ERα-positive breast cancers, activation of PKCα mediated by estrogen stimulation phosphorylates Ser39 of PHB2 (Nat. Commun., 8, 15427, 2017); therefore, PKCα activity state in ESR1 mutant breast cancer cell lines was evaluated. In the experiment, HEK293T cells and MCF-7 cells transfected with each ESR1 mutant were treated for 24 hours with PKCα inhibitor staurosporine, and immunoprecipitated with an anti-PKCα antibody. Then, PKCα activities were measured using the PHB2 peptide carrying Ser39 (YGVRESVFTVE (SEQ ID NO: 17)) as the substrate. As a result, while ESR1 mutant cells showed remarkable PKCα activity compared to mock and WT (Fig. 10A), staurosporine treatment nearly completely suppressed this activity (Fig. 10A), suggesting the possibility that the PKCα activity in ESR1 mutant cells is derived from PI3K.

Therefore, PKCα activity and phosphorylated PI3K, when MCF-7 cells transfected with various ESR1 mutants were treated for 24 hours with PI3K inhibitor wortmannin, were evaluated. As a result, the PKCα activities of the cells transfected with various ESR1 mutants were significantly suppressed by wortmannin treatment (Fig. 10B). Furthermore, in cells transfected with an ESR1 mutant, phosphorylation of PKCα and PI3K were remarkably induced than that in the WT. However, since each of these phosphorylations were nearly completely inhibited by wortmannin (Fig. 10C), activation of PKCα was suggested to be present downstream of PI3K. Furthermore, the PKCα activity and the intensity of phosphorylated PKCα in each ESR1 mutant cell line nearly correlated with each other, and the Y537S-transfected cell line showed the highest activation and phosphorylation of PKCα.

[0096]

Effects of Combined Use of stERAP and an Anti-estrogen Agent on the Growth of an ESR1 Mutant Breast Cancer Cell Line

Effects of combined use of stERAP with an existing hormone agent (tamoxifen or fulvestrant) or a molecularly-targeted drug (everolimus which is a mTOR inhibitor) on the growth of MCF-7 cells made to overexpress an ESR1 mutant, were examined in a 96-hour reaction. In the experiment, transfection of each ESR1 mutant in the absence of estrogen was followed by treatment with 10 μM stERAP, 1 μM tamoxifen, 2 μM fulvestrant, and 0.5 μM everolimus. As a result, 96-hour treatment with stERAP alone significantly suppressed the growth of ESR1 mutant-transfected cells, and in particular, inhibition rate of 49% was indicated by the Y537S mutant (Fig. 11). Furthermore, combined use of tamoxifen, fulvestrant, and everolimus was able to synergistically suppress the cell growth of the ESR1 mutants, and showed inhibition rates of 80% or more for the growth of all mutant cell lines (Fig. 11).

[0097]

Inhibitory Effects of stERAP on Growth of ESR1 Mutant Breast Cancer Cell Line in the Presence of Estrogen

stERAP treatment in the absence of estrogen showed 40% to 50% inhibition rate on the growth of a cell line transfected with an ESR1 mutant (Fig. 11); therefore, whether the inhibitory effects of stERAP in the presence of estrogen will be enhanced was examined. As a result, treatment with stERAP alone in the absence of estrogen hardly suppressed the cell growth of mock and WT, whereas inhibition rates of 24%, 44%, 39%, and 40% were indicated for the cell growth of the S463P, Y537S, D538G, and S463P/D538G mutants, respectively (Fig. 12). On the other hand, stERAP treatment in the presence of estrogen could nearly completely suppress estrogen-stimulated growth in mock and WT, and in each of the ESR1 mutants, co-presence of estrogen at 1 nM or higher caused synergistic enhancement of the inhibitory effects of stERAP, and inhibition rates of 62%, 80%, 75%, and 77% were indicated for the S463P, Y537S, D538G, and S463P/D538G mutants, respectively (Fig. 12). Furthermore, in the co-presence of 10 nM estrogen, the inhibition rates were found to be enhanced, and the inhibition rates were 76%, 82%, 84%, and 83%, respectively (Fig. 12). Here, the possibility was considered that addition of an estrogen signal increased the sites of action of stERAP, and synergistic inhibitory effects were induced.

[0098]

Inhibitory Effects of stERAP on ERα Transcriptional Activity in ESR1 Mutant Breast Cancer Cell Lines

Inhibitory effects of stERAP on ERα transcriptional activity in ESR1 mutants (S463P, Y537S, D538G, and S463P+D538G) were examined. In the experiment MCF-7 cells transfected with ERE-luciferase and each of the FLAG-tagged ESR1 mutants were treated for 24

hours with stERAP in the presence of estrogen at various concentrations (0.1 nM, 1 nM, or 10 nM), and the resulting ERE-luciferase activities (ERα transcriptional activities) were measured. As a result, in cells transfected with WT FLAG-tagged ERα, ERE-luciferase activity increased in a concentration-dependent manner when estrogen concentration was 0.1 nM or higher; however, this activity was nearly completely suppressed by stERAP treatment (Fig. 13). On the other hand, in cells transfected with each ESR1 mutant, ERE-luciferase activity was remarkably induced even in the absence of estrogen (S463P: 2.3-fold; Y537S: 7.5-fold; D538G: 5.0-fold; and S463P/D538G: 6.6-fold), and in particular, cells transfected with Y537S showed induction of activity at the same level as 10 nM estrogen stimulation of WT-transfected cells (Fig. 13). Furthermore, similarly to estrogen stimulation of the WT case, stERAP could remarkably suppress ERE-luciferase activities under any of the conditions.

[0099]

Inhibitory Effects of stERAP on Growth of Y537S Knocked-in MCF-7 Cells

MCF-7 cells knocked-in with Y537S of ESR1 were used to examine the effects of a 24-hour stERAP treatment on cell growth. As a result, stERAP treatment suppressed cell growth in a concentration-dependent manner even in the absence of estrogen, showed significant inhibitory effects at 10 μM (Fig. 14), and the IC_{50} (50% inhibitory concentration) was 1.57 μM. Furthermore, in the presence of estrogen, addition of the estrogen signal significantly enhanced the inhibition rate by stERAP, and the IC_{50} was 0.78 μM.

[0100]

[Example 4] Effects of stERAP on Trastuzumab-resistant HER2-positive Breast Cancer Cells

Materials and Methods

Cell lines

Human breast cancer cell lines (MCF-7, BT-474, and SK-BR-3) were purchased from American Type Culture Collection (ATCC, Rockville, MD, USA). KPL-4 was provided by Dr. Junichi Kurebayashi (Kawasaki Medical School, Okayama, Japan) based on a Material Transfer Agreement, and trastuzumab-resistant SK-BR-3 was provided by Dr. Hirotaka Kanzaki (Okayama University, Okayama, Japan). All cell lines were cultured under conditions recommended by their respective depositors.

[0101]

Cell Culture

SK-BR-3 cells were cultured in McCoy'A (Thermo Fisher Scientific) supplemented with 10% FBS (Nichirei Biosciences Inc., Tokyo, Japan) and 1% antibiotic/antimycotic solution (Thermo Fisher Scientific, Fremont, CA, USA), and KPL-4 cells, BT-474 cells, and trastuzumab-resistant SK-BR-3 cells were cultured in DMEM (Sigma, St. Louis, MO, USA) supplemented with 10% FBS and 1% antibiotic/antimycotic solution. The cells were seeded into 48-well

plates (2 x 10^4 cells/0.2 mL), 6-well plates (5 x 10^5 cells/2 mL), or 10-cm dishes (2 x 10^6 cells/10 mL), incubated under 5% CO_2 at 37°C, and 24 hours later, treated with an inhibitor such as stERAP.

[0102]

Compounds and Inhibitors

For the peptide inhibiting the BIG3-PHB2 binding, the single stapled ERAP (stERAP) described in WO 2013/018690 was used. Recombinant PHB2 was purchased from Abnova (Taipei, Taiwan), recombinant TTK and recombinant MK5 were purchased from SignalChem (Richmond, Canada), and TTK inhibitor AZ3146 was purchased from Santa Cruz Biotechnology.

[0103]

Western Blot Analyses

Cells were lysed in a lysis buffer (50 mM Tris-HCl: pH 8.0, 150 mM NaCl, 0.1% NP-40, 0.5% CHAPS) containing 0.1% protease inhibitor cocktail III (Calbiochem, San Diego, CA, USA). The cell lysates were electrophorased, transferred to nitrocellulose membranes by blotting, and then the membranes were blocked with 4% BlockAce solution (Dainippon Pharmaceutical, Osaka, Japan) for 3 hours. The membranes were incubated for 12 hours in the presence of anti-BIG3 purified antibody (anti-hA7322 (His13), Sigma); anti-HA tag antibody (3F10, Roche, Mannheim, Germany); anti-PHB2 antibody, and anti-NcoR antibody (Abcam, Cambridge, UK); anti-PKAα cat antibody (C-20), anti-PKCα antibody (H-7), anti-PP1Cα antibody (FL-18), and anti-HDAC1 antibody (H-51) (Santa Cruz Biotechnology, Santa Cruz, CA, USA); anti-HER2 antibody (Merck, Darmstadt, Germany); anti-HER3 antibody (1B2E), anti-TTK antibody (D-8), anti-MK5 antibody (D70A10), anti-CHK1 antibody (G-4), anti-phosphorylated Shc (Y239/Y240), anti-p38 antibody, anti-phosphorylated p38 antibody (T180/Y182), anti-NF-κB p65 antibody, anti-IκB antibody (L35A5), and anti-phosphorylated IκB antibody (S32/S36, 5A5) (Cell Signaling Technology, Danvers, MA, USA); anti-Shc antibody (BD, Franklin Lakes, NJ, USA); anti-phosphorylated PHB2 purified antibody (Ser39), anti-phosphorylated BIG3 purified antibody (Ser305), and anti-phosphorylated BIG3 antibody (Ser1208, Scrum Inc., Tokyo, Japan); and anti-phosphorylated threonine antibody (Thermo Fisher Scientific). After incubation in the presence of HRP-conjugated secondary antibody (Santa Cruz Biotechnology) for 1 hour, the membranes were developed with an enhanced chemiluminescence system (GE Healthcare, Buckinghamshire, UK). The blots were scanned using the Image Reader LAS-3000 mini (Fujifilm, Tokyo, Japan).

[0104]

Phos-tag SDS-PAGE

Phos-tag SDS-PAGE was carried out using precast SuperSep gels (50 μM phos-tag acrylamide and 100 μM $ZnCl_2$, Wako Pure Chemical, Osaka, Japan) to evaluate the direct

phosphorylation of PHB2 by a kinase. WIDE-VIEW Prestained Protein Size Marker III (Wako Pure Chemical) was used as the molecular marker. Phosphorylation efficiencies were calculated from the ratio of the phosphorylated PHB2 band with respect to the total PHB2 band.

[0105]

Immunoprecipitation

As mentioned in the "Western Blot Analyses" section, the cells were lysed in a 0.1% NP-40 lysis buffer, and the cell lysates were pre-cleared with Normal IgG and rec-Protein G Sepharose 4B (Thermo Fisher Scientific) at 4°C for 3 hours. After centrifugation, the supernatants were incubated at 4°C for 12 hours in the presence of 5 μg of anti-BIG3 antibody, anti-PHB2 antibody, anti-HER2 antibody, anti-PKCα antibody, and anti-HA tag antibody. Then upon adding rec-Protein G Sepharose 4B and incubating at 4°C for 1 hour, the antigen-antibody complexes were precipitated. The immunoprecipitated protein complexes were washed three times with the lysis buffer, and separation was performed by SDS-PAGE. Thereafter, Western blot analyses were carried out.

[0106]

In Vivo Tumor Growth Inhibition

KPL-4 cell suspensions and trastuzumab-resistant SK-BR-3 cell suspensions (1×10^7 cells/mouse) were mixed with an equal volume of Matrigel (BD) and injected into the mammary fat pads of 5-week-old female BALB/c nude mice (Charles River Laboratories, Tokyo, Japan). The mice were reared in a pathogen-free isolation facility with a 12-hour light/dark cycle and were fed rodent chow and water *ad libitum*. The tumors were grown over one week until they reached sizes of approximately 100 mm^3 [calculated as 1/2 x (width x $length^2$)]. The mice were then randomized into each of the experiment groups (five heads/group). stERAP treatment involved administration of 150 μg/kg to mice by tail vein injection every seven days. The tumor volume was measured with calipers every four days for four weeks. All the experiments were performed in accordance with the guidelines of the animal facility at Tokushima University.

[0107]

Kinase Reaction

The activities of protein kinase A (PKA) and protein kinase C alpha (PKCα) were measured by reacting the immunoprecipitates of BIG3 and PKCα with a synthetic substrate CREBtide (KRREILSRRPSYR) and 0.5 mM ATP in a kinase buffer (25 mM Hepes, pH 7.2, 25 mM $MgCl_2$, 5 mM EDTA, 5 mM EGTA, 0.25 mM DTT) at 30°C for 30 minutes, and by using an ADP-Glo kinase assay Kit (Promega, Fitchburg, WI, USA).

[0108]

PP1Cα Activity

The phosphatase activity of PP1Cα was determined using the Protein Phosphatase

Assay Kit (AnaSpec, Fremont, CA, USA). After cell lysates were incubated with a substrate (*p*-Nitrophenyl phosphate) at room temperature for 60 minutes, the reaction was stopped and the absorbance at 405 nm was measured. PP1Cα activity (μmole/min) was defined as the amount of enzyme needed to catalyze 1 μmole of substrate per minute.

[0109]

Cell Growth Assay

Cell growth assay was carried out using the Cell Counting Kit-8 (CCK-8, Dojindo, Kumamoto, Japan). Cells were harvested, plated into 48-well plates at 2 x 10^4 cells/well, and maintained in an incubator (37°C) in the presence of 5% CO_2. At the point as instructed, a ten-fold diluted CCK-8 solution was added, this was incubated for 30 minutes, and the absorbance at 450 nm was measured to calculate the number of viable cells.

[0110]

Real-time PCR

The expression of BIG3 was evaluated by real-time PCR. Total RNA was extracted from each of the cells using NucleoSpin RNA (Macherey-Nagel, Germany), and this was reverse transcribed to cDNA using Superscript II reverse transcriptase (Thermo Fisher Scientific), oligo dT primer (Thermo Fisher Scientific), and 25 mM dNTP Mixture (Thermo Fisher Scientific). cDNA analyses were performed by real-time PCR on the 7500 Real Time PCR System (Thermo Fisher Scientific) using SYBR Premix Ex Taq (Thermo Fisher Scientific). Each sample was normalized to the mRNA content of β2-MG. The primers used for the amplification are as follows:

BIG3: 5'-CTTGACAAGGCCTTTGGAGT-3' (SEQ ID NO: 18) and
5'-CAATATGCTTTTCCCGCTTT-3' (SEQ ID NO: 19); and

β2-MG: 5'-AACTTAGAGGTGGGGAGCAG-3' (SEQ ID NO: 20) and
5'-CACAACCATGCCTTACTTTATC-3' (SEQ ID NO: 21).

[0111]

Isolation of Cytoplasm and Nucleus

The cytoplasmic fractions and nuclear fractions were isolated using NE-PER nuclear and cytoplasmic extraction reagent (Thermo Fisher Scientific).

[0112]

Cell Cycle

Cells were fixed using cold 70% ethanol, stained using 20 μg/mL propidium iodide (Sigma) and 1 mg/mL ribonuclease A (Sigma), and analyzed by FACS Calibur (BD, Franklin Lakes, NJ, USA). Cell cycle profiles were evaluated using CellQuest software (BD, Franklin Lakes, NJ, USA).

[0113]

Statistical Analysis

Student's t-tests were used to determine the statistical significance of the differences among the experimental groups. $P < 0.05$ was considered significant.

[0114]

Results

BIG3 in HER2-positive Breast Cancer Cell Lines Function as AKAP

The present inventors have reported in WO 2013/018690 and in Nat. Commun. 2017 May 30; 8: 15427 that BIG3 functions as an A kinase anchor protein (AKAP) in estrogen receptor (ERα)-positive breast cancer cells. This time, the present inventors examined whether BIG3 functions as AKAP in human epidermal growth factor receptor 2 (HER2)-positive breast cancer cell lines as well. First, BIG3 expressions in HER2-positive breast cancer cell lines were evaluated by real-time PCR. As a result, each of the HER2-positive breast cancer cell lines (BT-474 cells, SK-BR-3 cells, and KPL-4 cells) showed remarkable enhancement of BIG3 expression (Fig. 15A), and expression higher than in ERα-positive breast cancer MCF-7 cells was shown.

Accordingly, the inventors considered the possibility that BIG3 may function as AKAP in HER2-positive breast cancer cells as in ERα-positive breast cancer cells. As a result, in HER2-positive breast cancer cell lines SK-BR-3 cells and KPL-4 cells, PKA, PP1Cα, and PHB2 were found to bind strongly to the immunoprecipitates of BIG3 (Fig. 15B), and the possibility was considered that BIG3 may function as AKAP in HER2-positive breast cancer cells as well, by forming complexes with PKA and protein phosphatase.

Next, to evaluate the mechanism of BIG3 activation in HER2-positive breast cancer cells, whether PKA and PP1Cα exist downstream of the HER2 signal and Epidermal Growth Factor Receptor (EGFR) signal was investigated by examining the effects of BIG3 on PKA activity and PP1Cα activity using the HER2 inhibitor trastuzumab and the EGFR inhibitor lapatinib. As a result, treatment of the immunoprecipitates of BIG3 with the PKA inhibitor H-89 and trastuzumab showed inhibition rates of 100% and 88%, respectively, for PKA activity and inhibition rates of 96% and 88%, respectively, for PP1Cα activity (Fig. 15C). On the other hand, since lapatinib treatment showed decrease in PKA activity and PP1Cα activity by only about 15% (Fig. 15C), BIG3 was suggested to be activated *via* HER2 signaling.

[0115]

Mechanism of BIG3 Activation in HER2-positive Breast Cancer Cell Lines

Since phosphorylation of Ser305 and Ser1208 is necessary for the activation of BIG3 (Nat. Commun., 8, 15427, 2017), phosphorylation of BIG3 in HER2-positive breast cancer cells was examined. As a result, each of the phosphorylations (at Ser305 and at Ser1208) of BIG3 were found to be constitutively induced in SK-BR-3 cells and KPL-4 cells (Fig. 16), and BIG3

was considered to be constantly activated in HER2-positive breast cancer cells. On the other hand, when effects by PKA inhibitor H-89, HER2 inhibitor trastuzumab, and EGFR inhibitor lapatinib were examined, each of the phosphorylations (at Ser305 and at Ser1208) of BIG3 activated in SK-BR-3 cells and KPL-4 cells were nearly completely suppressed by treatment with H-89 and trastuzumab whereas lapatinib treatment was not so involved in the suppression of BIG3 phosphorylation (Fig. 16). This suggested that BIG3 may be activated *via* PKA derived from HER2 signaling.

[0116]

BIG3 in HER2-positive Breast Cancer Cell Lines Regulates the Inhibitory Activity of PHB2

So far, the present inventors have elucidated that phosphorylation of BIG3 activated by PKA enhances the phosphatase activity of PP1Cα, and that by dephosphorylating the phosphorylated Ser39 of the cancer suppressor PHB2 (Prohibitin 2) which is bound to BIG3, which is the regulation unit of PP1Cα, the phosphorylation is greatly involved in the growth of breast cancer cells (Nat. Commun., 8, 15427, 2017). Furthermore, the present inventors designed ERAPs which are dominant negative peptides targeting the BIG3-PHB2 interaction (Nat. Commun., 4, 2443, 2013), undertook biological improvements so that they will exhibit long-term stability and have high sensitivity to inhibition of BIG3-PHB2 interactions, and produced stapled ERAPs (stERAPs) (Sci. Rep., 7, 1821, 2017). Actually, when stERAP was administered to breast cancer cell lines, binding between BIG3 and PHB2 was completely inhibited, and PHB2 dissociated from BIG3 was rapidly phosphorylated at its Ser39, and showed its suppressive activity (Sci. Rep., 7, 1821, 2017). Then, the effects of stERAP on BIG3 and PHB2 in HER2-positive breast cancer cells were investigated. As a result, when SK-BR-3 cells and KPL-4 cells were treated with stERAP, the interaction between BIG3 and PHB2 was observed to be nearly completely inhibited (Fig. 17A). Furthermore, phosphorylation of Ser39 and threonine in PHB2 which dissociated from BIG3 as a result of stERAP treatment was found to be induced rapidly (Fig. 17A), and BIG3 was suggested to regulate the phosphorylation (suppressive activation) of PHB2.

Next, the mechanism of PHB2 activation in HER2-positive breast cancer cells was evaluated. The experiments were performed by examining suppression of PKA expression by the siRNA method to suppress activation of BIG3, and phosphorylation of PHB2 using the HER2 inhibitor trastuzumab and the EGFR inhibitor lapatinib. As a result, decreasing trend in phosphorylation of PHB2 (Ser39) was hardly observed by the siPKA treatment and trastuzumab treatment; however, the phosphorylation was nearly completely suppressed by the lapatinib treatment (Fig. 17B). Therefore, phosphorylation of PHB2 (Ser39) was considered to be mainly due to EGFR signaling.

On the other hand, since threonine phosphorylation in PHB2 was independent of HER2

signaling and EGFR signaling (Fig. 17B), an activation mechanism completely different from that of Ser39 phosphorylation was considered to exist.

[0117]

PKCα-dependent Phosphorylation of PHB2 (Ser39)

To date, since the present inventors have found that PKCα phosphorylates Ser39 of PHB2 in ERα-positive breast cancer (Nat. Commun., 8, 15427, 2017), the effects of suppressing PKCα expression by the siRNA method on the phosphorylation of PHB2 (Ser39) were examined. As a result, phosphorylation of PHB2 (Ser39) induced by stERAP treatment was remarkably suppressed by siPKCα treatment (Fig. 18A). Furthermore, since PKCα activity of the immunoprecipitates of PKCα in SK-BR-3 cells showed activity inhibition of approximately 80% by lapatinib treatment (Fig. 18B), PHB2 (Ser39) was suggested to be phosphorylated *via* PKCα activation caused by EGFR signaling.

[0118]

Phosphorylated PHB2 (Ser39) Suppressed Transcriptional Activity in the Nucleus

Involvement of PHB2 (Ser39) phosphorylation in suppression of transcriptional activity was evaluated using the phosphorylated mutant of PHB2. In the experiment, SK-BR-3 cells in which PHB2 expression has been suppressed by the siRNA method were transfected with HA-tagged PHB2 construct and the alanine mutant at Ser39 (S39A). 48 hours later, this was treated with stERAP for 24 hours. The nuclear fractions were isolated and immunoprecipitated with an HA antibody. As a result, the HA-tagged PHB2 that had translocated into the nucleus by stERAP treatment showed remarkable binding between transcriptional repressors NcoR and HDAC1 (Fig. 19A), suggesting that transcriptional activity may be suppressed. On the other hand, since binding of NcoR and HDAC1 to HA-tagged S39A was attenuated in S39A-transfected cells (Fig. 19A; reduction rate of 82% for NcoR and 54% for HDAC1), serine phosphorylation of PHB2, particularly Ser39 phosphorylation, was suggested to be greatly involved in the suppression of transcriptional activity. Furthermore, when the effects of Ser39 phosphorylation on suppression of transcriptional activity was examined using the phosphomimetic S39E, the cells transfected with the mock-phosphorylated S39E bound strongly to NcoR and HDAC1 as in WT (Fig. 19A), and phosphorylation of Ser39 in PHB2 was considered to be important for suppression of transcriptional activity.

Next, the effects of phosphorylation of PHB2 (Ser39) on the HER2-HER3 and HER2-Shc interactions were examined. As a result, Ser39 of PHB2 which had dissociated from BIG3 by treatment with stERAP alone was found to be phosphorylated, and by binding to HER2, it was shown to inhibit the interactions between HER2 and HER3 and between HER2 and Shc by 83% in both cases (Fig. 19B). On the other hand, while lapatinib treatment in the presence of stERAP hardly showed PHB2 (Ser39) phosphorylation, as described above (Fig. 17B), HER2-

HER3 and HER2-Shc interactions could be remarkably inhibited to 62% and 74%, respectively, and PHB2 (Ser39) phosphorylation was considered not to affect suppression of HER2 signaling. On the other hand, PHB2 was observed to also induce threonine phosphorylation by stERAP treatment (Fig. 19B). Since this phosphorylation was independent of HER2 signaling and EGFR signaling (Fig. 17B and Fig. 19B), this suggested the possibility that threonine phosphorylation of PHB2 is greatly involved in suppression of HER2 signaling.

[0119]

Threonine Phosphorylation of PHB2 and Its Activation Mechanism

The activation mechanism of threonine phosphorylation of PHB2 was examined. First, PHB2 threonine phosphorylation was evaluated when PKCα expression was suppressed by the siRNA method, assuming involvement of PKCα in a similar manner to Ser39 phosphorylation. PHB2 threonine phosphorylation induced by stERAP treatment was strongly maintained even in cells subjected to trastuzumab treatment and siPKCα treatment (Fig. 20A), suggesting that PHB2 threonine phosphorylation is activated by a kinase(s) other than PKCα.

PHB2 dissociated from BIG3 due to stERAP treatment was suggested to induce threonine phosphorylation in addition to phosphorylation of Ser39 (Fig. 17B and Fig. 19B); therefore, the PHB2 threonine phosphorylation sites were predicted using a public database. As a result, by NetPhos 3.1 (http://www.cbs.dtu.dk/services/NetPhos/), Thr155 and Thr169 showed high scores (0.849 and 0.992, respectively; Table 1A). While they were both present in the inhibitory domain of the ERα transcriptional activity of PHB2 (19-49 aa and 150-174 aa; Proc. Natl. Acad. Sci. USA, 96, 6947, 1999), there suggested the possibility that Thr169 may be phosphorylated by a kinase other than PKC.

[0120]

[Table 1]

Threonine phosphorylation sites of PHB2 and kinases by public databases

A

Predicted sites of threonine phosphorylation in PHB2 (NetPhos 3.1)

Target site	Score	Kinase
T169	0.992	–
T155	0.849	PKC
T194	0.738	–
T94	0.617	PKC
T42	0.526	CKI
T62	0.476	CaM-II
T185	0.476	cdc2
T21	0.457	CaM-II
T288	0.455	GSK3
T274	0.452	CaM-II
T263	0.444	GSK3
T266	0.425	GSK3

B

Kinase predicted sites on threonine phosphorylation in PHB2 (GPS 3.0)

Phosphorylated site	Kinase	Score
T42	TTK	62.64
T194	GRK	14.28
T185	MAPK2K2	12.00
T169	CHK1	11.55
T62	TAOK1	11.00
T169	MK5	10.63
T288	GRK1	10.62
T266	PIM1	10.15
T155	MAP2K2	9.00
T263	MAP4K4	9.00
T21	VRK2	8.50
T274	AMPKA1	7.75
T94	AAK1	5.00

Next, when kinases involved in the phosphorylation of the threonine residue of PHB2 were predicted using the Group-based Prediction System (GPS3.0; http://gps.biocuckoo.org/), TKK showed a remarkably high score (62.64) compared to the other kinases with respect to Thr42 phosphorylation (Table 1B). From the above-mentioned prediction results, Thr42 and Thr169 of PHB2 were predicted to be the threonine phosphorylation sites, and the present inventors focused on TTK as the kinase for Thr42 and CHK1 and MK5 as the kinases for Thr169.

Then, PHB2 threonine phosphorylation was evaluated when stERAP treatment was performed by suppressing TTK, CHK1, and MK5 expressions by the siRNA method. As a result, when PHB2 threonine phosphorylation induced by stERAP treatment was subjected to siTTK treatment and siMK5 treatment, inhibitory effects of 79% and 74% were shown, respectively (Fig. 20B). Furthermore, while siCHK1 treatment showed an inhibition rate of 33% for threonine phosphorylation of PHB2, TTK and MK5 were determined to be greatly involved in the threonine phosphorylation of PHB2.

Since it has been reported that p38 is a substrate of TTK (JP 4647456 B2), the relationship between TTK and p38 was investigated. Interestingly, p38 phosphorylation was suppressed to approximately 25% by siTTK treatment (Fig. 20B), suggesting that p38 is present downstream of TTK. Furthermore, since p38 activates MK5 (Cell Signal, 22, 1185, 2010), this suggested the presence of a pathway in which MK5 is activated *via* p38 activated by TTK. From the above-mentioned results, it was considered that TTK regulates the phosphorylation of

Thr42 and Thr169 in PHB2, and that MK5 is involved in the phosphorylation of Thr169.

[0121]

Effects of Threonine Phosphorylation of PHB2 by TTK and MK5 on HER2 Signaling

To investigate the effects of TTK, MK5, and CHK1 on the HER2-HER3 and HER2-Shc interactions, the expression of each of them were suppressed by siRNA, and then immunoprecipitation was performed with a HER2 antibody. As a result, when SK-BR-3 cells were treated with 1 μM stERAP, binding of HER3 and Shc to HER2 were inhibited by 93% and 90%, respectively; whereas this binding inhibition was avoided when TTK expression and MK5 expression were suppressed (Fig. 21A; siTTK: inhibition rates of 23% and 9%, respectively; siMK5: inhibition rates of 48% and 31%, respectively). Furthermore, suppression of TTK expression and MK5 expression suppressed the threonine phosphorylation of PHB2 caused by stERAP treatment by 87% and 46%, respectively (Fig. 21A). Since similar results were also obtained from other HER2-positive breast cancer cell line KPL-4 cells (Fig. 21B), it was considered that threonine phosphorylation of PHB2 by TTK and MK5 is important for the regulation of the HER2 signaling cascade. On the other hand, since suppression of CHK1 expression in SK-BR-3 cells and KPL-4 cells could not avoid the inhibition of HER2-HER3 binding and HER2-Shc binding caused by stERAP treatment, CHK1 was considered to be hardly involved in HER2 signaling.

Next, by using the TTK inhibitor AZ3146, effects on threonine phosphorylation of PHB2 and HER2 signaling were examined. As a result, while treatment with stERAP alone could reproduce the remarkable inhibition of HER2-HER3 and HER2-Shc interactions (inhibition rates of 96% and 91%, respectively), AZ3146 nearly completely cancelled the inhibitory effects (Fig. 20C). Furthermore, since AZ3146 inhibited the threonine phosphorylation of PHB2 to 23% (Fig. 20C), this suggested that threonine phosphorylation of PHB2 caused by TTK activation is involved in the inhibition of HER2 signaling.

[0122]

Identification of the Threonine Phosphorylation Sites of PHB2

Whether the threonine phosphorylation sites of PHB2 are Thr42 and Thr169 was examined. In the experiment, SK-BR-3 cells in which the expression of endogenous PHB2 was suppressed by the siRNA method were transfected with the HA-tagged PHB2 construct (WT), alanine mutant at Thr42 (T42A), alanine mutant at Thr169 (T169A), and double alanine mutant at Thr42 and at Thr169 (T42A + T169A), and after treatment with stERAP for 24 hours, the cells were immunoprecipitated using an anti-HA antibody. As a result, threonine phosphorylation of PHB2 induced by stERAP treatment in WT-transfected cells was observed to be attenuated by 50% and 20% in the T42A and T169A mutants, respectively, and 76% of threonine phosphorylation was suppressed in the T42A + T169A double mutant (Fig. 22A).

Next, the effects of each of the phosphorylations at Thr42 and Thr169 of PHB2 on the suppression of HER2 signaling were examined. In the experiment, SK-BR-3 cells in which the expression of endogenous PHB2 was suppressed by the siRNA method were transfected with each HA-tagged PHB2 (wild type (WT), alanine mutant at Ser39 (S39A), and double alanine mutant at Thr42 and at Thr169 (T42A + T169A)), and after treatment with stERAP for 24 hours, the cells were immunoprecipitated using an anti-HER2 antibody and an anti-BIG3 antibody. As a result, while each HA-tagged PHB2 bound directly to HER2 even without stERAP treatment, stERAP treatment nearly completely inhibited the binding between BIG3 and each HA-tagged PHB2 (Fig. 22B, immunoprecipitants of BIG3), and since the amount of HA-tagged PHB2 bound to HER2 increased accordingly, it was judged that under stERAP treatment, conditions where HA-tagged PHB2 does not bind to BIG3 is established.

Therefore, under this condition, the effects of each HA-tagged PHB2 on the HER2-HER3 and HER2-Shc interactions were examined. PHB2-WT bound to HER2 nearly completely inhibited the HER2-HER3 and HER2-Shc interactions (Fig. 22B; inhibition rates of 98% for HER2-HER3 and 93% for HER2-Shc); whereas the binding with HER3 and Shc were inhibited by 95% and 85%, respectively, in the PHB2-S39A mutant (Fig. 22B), and the inhibitory effect was approximately the same as that in WT. On the other hand, in the T42A + T169A threonine double mutant, even though Ser39 of PHB2 was phosphorylated, the suppressive function of PHB2 was remarkably lost (inhibition rates of 15% for HER2-HER3 and 15% for HER2-Shc), suggesting that the suppressive function of PHB2 on HER2 signaling is greatly involved in the respective phosphorylation of Thr42 and Thr169.

[0123]

<u>Threonine Phosphorylation of PHB2 Caused by TTK and MK5</u>

Whether TTK and PHB2 bind was examined by immunoprecipitating SK-BR-3 cells treated for 24 hours with stERAP using an anti-TTK antibody and an anti-PHB2 antibody. As a result, immunoprecipitations with both antibodies showed that TTK and PHB2 strongly interact (Fig. 23A), suggesting that TTK directly phosphorylates PHB2.

Next, the possibility that TTK and MK5 directly threonine-phosphorylate PHB2 was evaluated by SDS-PAGE which uses Phos-tag. In the experiment, recombinant PHB2 and recombinant TTK or recombinant MK5 were reacted in the presence of ATP at 30°C for 30 minutes, and then subjected to Phos-tag SDS-PAGE. As a result, while a phosphorylation band was slightly observed (28% phosphorylation) when the molar ratio between recombinant TTK and PHB2 was 1:1, when the molar ratio was PHB2:TTK = 1:2 or greater, a band for 75% phosphorylation was clearly detected (Fig. 23B). When immunoblotting was performed using an anti-phosphorylated threonine antibody, phosphorylation bands were found at nearly the same positions (Fig. 23B). Furthermore, when immune serum against phosphorylated Thr42 and

phosphorylated Thr169 were immunoblotted, phosphorylated Thr42 was detected with high sensitivity, but depending on the molar ratios of PHB2 and TTK, each phosphorylation band was observed clearly (Fig. 23B), suggesting the possibility that TTK can directly phosphorylate Thr42 and Thr169 of PHB2.

Regarding recombinant MK5, a phosphorylation band was slightly observed (6.5% phosphorylation) starting from molar ratio of PHB2:MK5 = 1:0.25, the phosphorylation efficiency increased depending on the molar ratio, and at a molar ratio of PHB2:MK = 1:2 or more, a band for 75% phosphorylation was detected, and this band was at the same position as in the immunoblot of anti-phosphorylated threonine antibody (Fig. 23C). Furthermore, when immune serum was immunoblotted similarly to the method described above, serum of phosphorylated Thr42 slightly reacted, and phosphorylated Thr169 serum showed nearly the same phosphorylation manner as the anti-phosphorylated threonine antibody, and this strongly suggested that in PHB2, Thr169 is the site of phosphorylation by MK5.

[0124]

Inhibitory Effects of stERAP on the Growth of HER2-positive Breast Cancer Cell Lines

The growth suppressive effects of stERAP on HER2-positive breast cancer cell lines were examined (Fig. 24). As a result, stERAP showed dose-dependent inhibitory effects on the growth of each of the HER2-positive breast cancer cell lines (SK-BR-3 cells, BT-474 cells, and KPL-4 cells), and the IC_{50} (50% inhibition concentration) for the cell lines were 0.054 μM, 0.58 μM, and 0.02 μM, respectively. Furthermore, since SK-BR-3 cells and KPL-4 cells are estrogen receptor (ERα)-negative, stERAP was found to show remarkable growth suppressive effects in HER2-positive breast cancer cells and in ERα-negative cells as long as cells express BIG3.

[0125]

stERAP Inhibits the HER2-HER3 and HER2-Shc Interactions

Using the IC_{50} and complete inhibition concentration of stERAP for the growth of each of the HER2-positive breast cancer cell lines (SK-BR-3 cell: 0.05 μM and 1 μM; BT-474 cell: 0.5 μM and 10 μM; and KPL-4 cell: 0.01 μM and 1 μM, respectively), effects on the HER2-HER3 and HER2-Shc interactions in each cell line and effects of combined use with trastuzumab were examined. As a result, trastuzumab could hardly inhibit the binding of HER2 to HER3 and Shc whereas treatment with stERAP alone achieved strong inhibitory effects (Fig. 25), and at the complete inhibition concentration against cell growth, HER2-HER3 and HER2-Shc interactions could be inhibited nearly completely. Furthermore, when trastuzumab was used in combination with stERAP at its IC_{50}, dramatic enhancements in inhibition rates were observed (Fig. 25).

Furthermore, stERAP treatment showed similar inhibitory effects on the

phosphorylation of HER2 (Y877) and the phosphorylation of Shc (Y239/Y240) (Fig. 25). In addition, although stERAP treatment induced the binding level of PHB2 to HER2 in a concentration-dependent manner, combined use with trastuzumab did not change the binding level of PHB2 (Fig. 25).

[0126]

Inhibitory Effects of stERAP on Trastuzumab-resistant HER2-positive Breast Cancer Cell Lines

Growth inhibitory effects of stERAP on trastuzumab-resistant SK-BR-3 cell were examined. As a result, administration of trastuzumab alone could not suppress the growth of trastuzumab-resistant SK-BR-3 cells at all whereas stERAP treatment showed dose-dependent suppressive effects on the growth of trastuzumab-resistant SK-BR-3 cells. Compared to the IC_{50} (0.054 μM, Fig. 24) for trastuzumab-sensitive SK-BR-3 cells, the IC_{50} was 10.64 μM which was higher (Fig. 26A), but regardless of whether the cells are resistant or sensitive, stERAP was found to have significant suppressive effects.

Next, effects of stERAP on the binding of the HER2-HER3 heterodimer and HER2-Shc in trastuzumab-resistant SK-BR-3 cells were examined. As a result, stERAP could nearly completely inhibit the binding of HER2-HER3 and HER2-Shc and the phosphorylation of Shc (Y239/Y240) in the sensitive and resistant cell lines (Fig. 26B). Furthermore, PHB2 which dissociated from BIG3 by stERAP treatment was observed to bind to HER2, and PHB2 was suggested to be involved in the inhibition of HER2-HER3 and HER2-Shc complexes. On the other hand, treatment with Herceptin alone hardly affected the binding of HER2-HER3 and HER2-Shc.

[0127]

Effects of stERAP on NF-κB Signaling in Trastuzumab-resistant HER2-positive Breast Cancer Cell Lines

It has been reported the possibility that activation of NF-κB signaling in HER2-positive breast cancer cells causes resistance to chemoradiotherapy (Anticancer Res., 26, 4235, 2006; Breast Cancer Res., 13, 221, 2011). Therefore, the effects of stERAP on NF-κB signaling in HER2-positive breast cancer cell lines were examined. As a result, compared to the parent SK-BR-3 cell line cells, a lot of NF-κB p65 was found to translocate into the nucleus in trastuzumab-resistant SK-BR-3 cells, and this signal was suggested to be involved in the resistance against trastuzumab treatment (Fig. 27). On the other hand, administration of stERAP remarkably inhibited the nuclear translocation of NF-κB p65 in trastuzumab-resistant SK-BR-3 cells (Fig. 27). Furthermore, stERAP was found to regulate the nuclear translocation of NF-κB p65 by nearly completely inhibiting the phosphorylation of IκBα which is activated only in trastuzumab-resistant SK-BR-3 cells (Fig. 27). The above result suggests that stERAP can avoid resistance to trastuzumab treatment by suppressing phosphorylation of IκBα and nuclear

translocation of NF-κB p65.

[0128]

Effects of stERAP on the Cell Cycle of a Trastuzumab-resistant HER2-positive Breast Cancer Cell Line (Fig. 28)

Effects of stERAP administration on the cell cycle of trastuzumab-resistant SK-BR-3 cells were examined. As a result, the cell cycle of trastuzumab-resistant SK-BR-3 cells had remarkably progressed to the G2/M phase, and although administration of trastuzumab could hardly arrest the cell cycle, administration of stERAP alone was found to arrest the cell cycle at the G0/G1 phase. Furthermore, when 20 μM stERAP and 100 μg/mL trastuzumab were used in combination, cells at the sub-G1 phase remarkably increased, and cell death was observed. The above result revealed that stERAP induces cytostatic effects by inducing G1 phase arrest and promotes cell death when used in combination with trastuzumab which has a different action mechanism.

[0129]

In Vivo Antitumor Effects of stERAP on Trastuzumab-resistant HER2-positive Breast Cancer Cells (Fig. 29)

In vivo antitumor effects by stERAP were examined. KPL-4 and trastuzumab-resistant SK-BR-3 cells were orthotopically transplanted into the mammary glands of BALB/c nude mouse. When the tumor reached approximately 100 mm^3, stERAP administration through the tail vein was initiated, and then stERAP was administered every seven days thereafter, and the antitumor effects were investigated. As a result, while the KPL-4 tumor and the trastuzumab-resistant SK-BR-3 tumor grew over time, immediately after administration of stERAP at 150 μg/kg, the tumor size showed a decreasing trend, significant inhibitory effects were sustained even when administered every seven days, and tumor reduction was observed 28 days later. No toxicity and no significant body weight decrease due to stERAP administration were observed. Therefore, from a therapeutic viewpoint, excellent therapeutic index is suggested.

[0130]

[Example 5] Effects of Double stERAPs

Materials and Methods

Cell lines and Culture Conditions

Three types of human breast cancer cell lines SK-BR-3, BT-20, and MDA-MB-231, and a human synovial sarcoma cell line SW982 were purchased from American Type Culture Collection (ATCC, Manassas, VA, USA).

SK-BR-3 cells were cultured using McCoy's 5A medium (Thermo Fisher Scientific, Waltham, MA, USA), BT-20 cells were cultured using EMEM medium (Thermo Fisher Scientific) under 5% CO_2 at 37°C. MDA-MB-231 cells and SW982 cells were cultured using

Leibovitz's L-15 medium (Thermo Fisher Scientific) at 37°C without CO_2 concentration control. All media were used by supplementing 10% FBS (Thermo Fisher Scientific) and a 1% antibiotic/antimycotic solution (Wako Pure Chemical, Osaka, Japan).

[0131]

Cell Growth Assay

SK-BR-3 cells, BT-20 cells, and MDA-MB-231 cells were seeded into 48-well plates at 1 x 10^4 cells/200 μL in each well, and SW982 cells were seeded into 48-well plates at 0.5 x 10^4 cells/200 μL in each well. 48 hours later, the medium in each well was exchanged to a medium supplemented with a peptide (single stERAP and double stERAP #46: three-fold serial dilution from 20 μM, double stERAP #45: two-fold serial dilution starting from 50 μM), and after culturing for another 96 hours, the level of cell growth was measured using the Cell Counting Kit-8 (Dojindo, Kumamoto, Japan). Data were obtained from three independent experiments, a graph (mean ± standard deviation) was produced using a graphing and data analyzing software SigmaPlot (Systat Software, San Jose, CA, USA), and the 50% inhibition concentration (IC_{50}) of the peptide against cell growth was calculated.

[0132]

Cell Cycle Analysis

SK-BR-3 cells and MDA-MB-231 cells were seeded respectively at 5 x 10^5 cells/10 cm dish. 72 hours later, the medium was exchanged to a fresh medium supplemented with 5 μM peptide; cells were collected by trypsin treatment 48 hours, 72 hours, and 96 hours later; and the cells were fixed at -20°C overnight or longer by adding 70% ethanol solution. The solution for the cell suspension was exchanged from 70% ethanol to Propidium Iodide (PI)/RNase Staining Solution (Cell Signaling Technologies, Danvers, MA, USA), and after allowing the reaction to take place at room temperature in the dark for 15 minutes, the cell aggregates were removed using a cell strainer (BD biosciences, Franklin Lakes, NJ, USA). Next, the ratio of cell cycle phases for each cell sample was analyzed using FACS array (BD biosciences) and the analysis software FlowJo (FLOWJO LCC, Ashland, OR, USA).

[0133]

Results

Growth Inhibitory Effects of stERAPs on Breast Cancer Cell Lines and a Synovial Sarcoma Cell Line

The effects of three types of stERAPs on cell growth of three types of breast cancer cell lines (SK-BR-3, BT-20, and MDA-MB-231) and synovial sarcoma cell line SW982 were investigated. As a result, as shown in Fig. 30, concentration-dependent inhibitory effects on cell growth by each stERAP were observed in all cell lines. Furthermore, the 50% inhibition concentration (IC_{50}) for each peptide is shown in Table 2. Among the three types of peptides,

double stERAP #46 had the highest growth inhibitory effects and strong growth inhibitory effects were observed in the highly malignant triple negative breast cancer-derived cell lines (BT-20 and MDA-MB-231) and synovial sarcoma-derived cell line SW982.

[0134]

Effects of stERAPs on the Cell Cycle of Breast Cancer Cell Lines (SK-BR-3 and MDA-MB-231)

The effects of two types of peptides (single stERAP and double stERAP #46) having remarkable cytostatic effects on the cell cycles of two types of breast cancer cell lines (SK-BR-3 and MDA-MB-231) were examined by flow cytometry analyses. As a result, as shown in Fig. 31A, in SK-BR-3 cells, for both peptides, addition of peptide led to decrease in the number of cells at the G2/M phase and increase in the number of cells at the G1 phase, in comparison to a negative control in which phosphate-buffered saline (PBS) was added to cells. Accordingly, a G1-phase cell cycle arrest was observed. This effect was maintained even at 96 hours after peptide addition. On the other hand, in MDA-MB-231 cells, as shown in Fig. 31B, decrease in the number of G1-phase cells and increase in the number of S-phase cells were observed, S phase cell cycle arrest was observed, and these effects were maintained even 96 hours after peptide addition. These results suggest the possibility that the cytostatic effects of the two types of peptides (single stERAP and double stERAP #46) induce about cell cycle arrest.

[0135]

[Table 2]

50% Cell growth inhibition concentration of stERAP peptides (IC_{50}, μM)

Peptide	MDA-MB-231	BT-20	SK-BR-3	SW 982
Single stERAP	0.597	0.36	0.09	0.274
Double stERAP #45	23.7	8.6	2.8	Not performed
Double stERAP #46	0.143	0.074	0.02	0.026

[Industrial Applicability]

[0136]

The present invention provides peptides having longer lasting inhibitory effects on the BIG3-PHB2 interaction. Pharmaceutical compositions comprising a peptide of the present invention or a salt thereof can be used to treat cancer, and particularly estrogen receptor-positive cancers and estrogen receptor-negative breast cancers and prostate cancers.

Claims

1. A peptide comprising an amino acid sequence in which at least two pairs of amino acid residues are substituted with the same number of stapling structures in the amino acid sequence of SEQ ID NO: 4 or SEQ ID NO: 5, or a salt thereof,

wherein the two pairs of amino acid residues are either (a) and (b), or (c) and (d) below:

(a) the third and seventh amino acid residues from the N terminus of the amino acid sequence of SEQ ID NO: 4; and

(b) the eighth and twelfth amino acid residues from the N terminus of the amino acid sequence of SEQ ID NO: 4, or

(c) the third and seventh amino acid residues from the N terminus of the amino acid sequence of SEQ ID NO: 5; and

(d) the tenth and fourteenth amino acid residues from the N terminus of the amino acid sequence of SEQ ID NO: 5.

2. The peptide or the salt thereof of claim 1, wherein two pairs of amino acid residues are substituted with two stapling structures.

3. The peptide or the salt thereof of claim 1, wherein the stapling structure is represented by Formula (I) below:

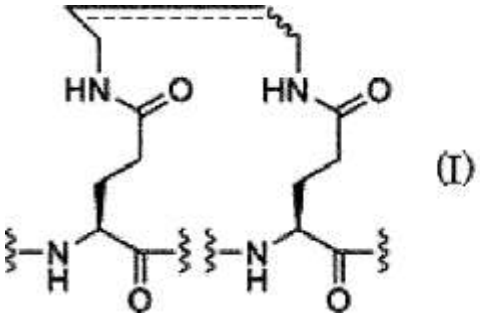

(I)

(wherein, the double line drawn by a solid line and a dashed line indicates a single bond or a double bond).

4. The peptide or the salt thereof of claim 3, wherein the stapling structure is represented by Formula (II) below:

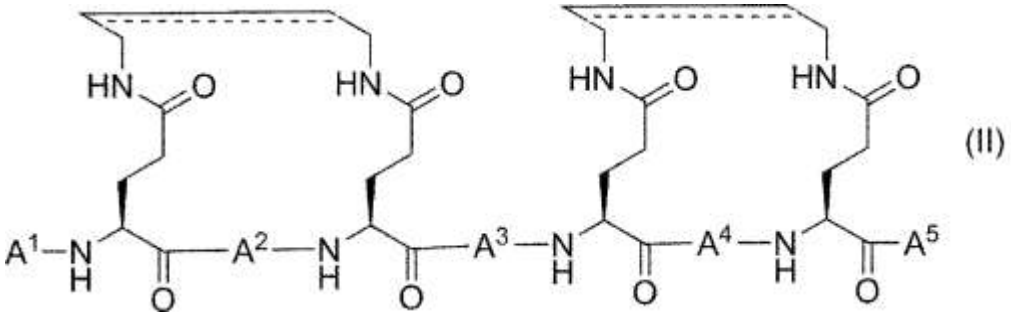

(II)

(wherein, the double line drawn by a solid line and a dashed line indicates a single bond or a double bond;

the combination of A^1, A^2, A^3, A^4, and A^5 is selected from the following:

A^1 = QM, A^2 = SDL, A^3 = –, A^4 = QLR, and A^5 = R; and

A^1 = QM, A^2 = SDL, A^3 = LQ, A^4 = RQR, and A^5 = OH;

wherein "–" indicates a peptide bond with no additional amino acid residue (that is, two stapling structures are connected); and "OH" indicates that one end of the above stapling structure constitutes the C terminus of the peptide derivative).

5. The peptide or the salt thereof of claim 1, wherein either one or both of N-terminal and C-terminal amino acid residues have been modified.

6. The peptide or the salt thereof of claim 5, wherein either one or both of N-terminal and C-terminal amino acid residues have been modified by any one or a combination of acetylation, amidation, and HA tagging.

7. The peptide or the salt thereof of claim 6, wherein the N-terminal amino acid residue is acetylated and the C-terminal amino acid residue is amidated.

8. The peptide or the salt thereof of claim 1, wherein all the amino acid residues have been substituted with D-form amino acid residues.

9. A peptide which is a retro-inverso form of a peptide comprising an amino acid sequence in which at least two pairs of amino acid residues are substituted with the same number of stapling structures in the amino acid sequence of SEQ ID NO: 4 or SEQ ID NO: 5, or a salt thereof, wherein the two pairs of amino acid residues are (a) and (b) below:

(a) the third and seventh amino acid residues from the N terminus of the amino acid sequence of SEQ ID NO: 4; and

(b) the eighth and twelfth amino acid residues from the N terminus of the amino acid sequence of SEQ ID NO: 4, or

wherein the two pairs of amino acid residues are (c) and (d) below:

(c) the third and seventh amino acid residues from the N terminus of the amino acid sequence of SEQ ID NO: 5; and

(d) the tenth and fourteenth amino acid residues from the N terminus of the amino acid sequence of SEQ ID NO: 5.

10. A pharmaceutical composition comprising the peptide or the salt thereof of claim 1 and a pharmaceutically acceptable carrier.

11. Use of the pharmaceutical composition of claim 10 in the manufacture of a medicament for treating cancer.

12. The use of claim 11, wherein the cancer is breast cancer or prostate cancer.

13. The use of claim 11, wherein the cancer is estrogen receptor-positive cancer.